

# Metadata of the article that will be visualized in OnlineFirst

---

|              |  |
|--------------|--|
| ArticleTitle | Nodulation in the absence of <i>nod</i> genes induction: alternative mechanisms involved in the symbiotic interaction between <i>Cupriavidus</i> sp. UYMMa02A and <i>Mimosa pudica</i> |
|--------------|--|

---

Article Sub-Title

---

|                   |   |
|-------------------|---|
| Article CopyRight | The Author(s) under exclusive licence to Society for Environmental Sustainability<br>(This will be the copyright line in the final PDF) |
|-------------------|---|

---

|              |                              |
|--------------|------------------------------|
| Journal Name | Environmental Sustainability |
|--------------|------------------------------|

---

|                      |              |   |
|----------------------|--------------|---|
| Corresponding Author | FamilyName   | <b>Platero</b>  |
|                      | Particle     |   |
|                      | Given Name   | <b>Raúl A.</b>  |
|                      | Suffix       |   |
|                      | Division     | Laboratorio de Microbiología Ambiental. Departamento de Bioquímica y Genómica Microbianas, Instituto de Investigaciones Biológicas Clemente Estable |
|                      | Organization | Ministerio de Educación y Cultura   |
|                      | Address      | Montevideo, Uruguay   |
|                      | Phone        |   |
|                      | Fax          |   |
|                      | Email        | rplatero@iibce.edu.uy   |
|                      | ORCID        | <a href="http://orcid.org/0000-0001-5331-1396">http://orcid.org/0000-0001-5331-1396</a>   |

---

|        |              |   |
|--------|--------------|---|
| Author | FamilyName   | <b>Rodríguez-Esperón</b>  |
|        | Particle     |   |
|        | Given Name   | <b>Cecilia</b>  |
|        | Suffix       |   |
|        | Division     | Laboratorio de Microbiología Ambiental. Departamento de Bioquímica y Genómica Microbianas, Instituto de Investigaciones Biológicas Clemente Estable |
|        | Organization | Ministerio de Educación y Cultura   |
|        | Address      | Montevideo, Uruguay   |
|        | Phone        |   |
|        | Fax          |   |
|        | Email        |   |
|        | ORCID        |   |

---

|        |              |   |
|--------|--------------|---|
| Author | FamilyName   | <b>Sandes</b>   |
|        | Particle     |   |
|        | Given Name   | <b>Laura</b>  |
|        | Suffix       |   |
|        | Division     | Laboratorio de Microbiología Ambiental. Departamento de Bioquímica y Genómica Microbianas, Instituto de Investigaciones Biológicas Clemente Estable |
|        | Organization | Ministerio de Educación y Cultura   |
|        | Address      | Montevideo, Uruguay   |
|        | Phone        |   |
|        | Fax          |   |
|        | Email        |   |
|        | ORCID        |   |

---

|        |              |   |
|--------|--------------|---|
| Author | FamilyName   | <b>Eastman</b>  |
|        | Particle     |   |
|        | Given Name   | <b>Ignacio</b>  |
|        | Suffix       |   |
|        | Division     | Laboratorio de Microbiología Ambiental. Departamento de Bioquímica y Genómica Microbianas, Instituto de Investigaciones Biológicas Clemente Estable |
|        | Organization | Ministerio de Educación y Cultura   |
|        | Address      | Montevideo, Uruguay   |
|        | Phone        |   |
|        | Fax          |   |
|        | Email        |   |
|        | URL          |   |
|        | ORCID        |   |
| Author | FamilyName   | <b>Croci</b>  |
|        | Particle     |   |
|        | Given Name   | <b>Carolina</b>   |
|        | Suffix       |   |
|        | Division     | Laboratorio de Microbiología Ambiental. Departamento de Bioquímica y Genómica Microbianas, Instituto de Investigaciones Biológicas Clemente Estable |
|        | Organization | Ministerio de Educación y Cultura   |
|        | Address      | Montevideo, Uruguay   |
|        | Division     | Laboratorio de Ecología Microbiana Acuática, Departamento de Microbiología, Instituto de Investigaciones Biológicas Clemente Estable                |
|        | Organization | Ministerio de Educación y Cultura   |
|        | Address      | Montevideo, Uruguay   |
|        | Phone        |   |
|        | Fax          |   |
|        | Email        |   |
|        | URL          |   |
|        | ORCID        |   |
| Author | FamilyName   | <b>Garabato</b>   |
|        | Particle     |   |
|        | Given Name   | <b>Florencia</b>  |
|        | Suffix       |   |
|        | Division     | Laboratorio de Microbiología Ambiental. Departamento de Bioquímica y Genómica Microbianas, Instituto de Investigaciones Biológicas Clemente Estable |
|        | Organization | Ministerio de Educación y Cultura   |
|        | Address      | Montevideo, Uruguay   |
|        | Phone        |   |
|        | Fax          |   |
|        | Email        |   |
|        | URL          |   |
|        | ORCID        |   |
| Author | FamilyName   | <b>Ferreira</b>   |
|        | Particle     |   |
|        | Given Name   | <b>Virginia</b>   |
|        | Suffix       |   |
|        | Division     | Laboratorio de Microbiología Ambiental. Departamento de Bioquímica y Genómica Microbianas, Instituto de Investigaciones Biológicas Clemente Estable |
|        | Organization | Ministerio de Educación y Cultura   |
|        | Address      | Montevideo, Uruguay   |
|        | Phone        |   |
|        | Fax          |   |
|        | Email        |   |
|        | URL          |   |
|        | ORCID        |   |

---

|        |              |                  |
|--------|--------------|------------------|
| Author | FamilyName   | <b>Baraiibar</b> |
|        | Particle     |                  |
|        | Given Name   | <b>Martín</b>    |
|        | Suffix       |                  |
|        | Division     |                  |
|        | Organization | OXIProteomics    |
|        | Address      | Créteil, France  |
|        | Phone        |                  |
|        | Fax          |                  |
|        | Email        |                  |
|        | URL          |                  |
|        | ORCID        |                  |

---

|        |              |   |
|--------|--------------|---|
| Author | FamilyName   | <b>Portela</b>  |
|        | Particle     |   |
|        | Given Name   | <b>Magdalena</b>  |
|        | Suffix       |   |
|        | Division     | Unidad Mixta de Bioquímica y Proteómica Analíticas, Institut Pasteur de Montevideo-Instituto de Investigaciones Biológicas Clemente Estable |
|        | Organization | Ministerio de Educación y Cultura   |
|        | Address      | Montevideo, Uruguay   |
|        | Division     | Facultad de Ciencias  |
|        | Organization | Universidad de la República   |
|        | Address      | Montevideo, Uruguay   |
|        | Phone        |   |
|        | Fax          |   |
|        | Email        |   |
|        | URL          |   |
|        | ORCID        |   |

---

|        |              |   |
|--------|--------------|---|
| Author | FamilyName   | <b>Durán</b>  |
|        | Particle     |   |
|        | Given Name   | <b>Rosario</b>  |
|        | Suffix       |   |
|        | Division     | Unidad Mixta de Bioquímica y Proteómica Analíticas, Institut Pasteur de Montevideo-Instituto de Investigaciones Biológicas Clemente Estable |
|        | Organization | Ministerio de Educación y Cultura   |
|        | Address      | Montevideo, Uruguay   |
|        | Phone        |   |
|        | Fax          |   |
|        | Email        |   |
|        | URL          |   |
|        | ORCID        |   |

---

|          |          |             |
|----------|----------|-------------|
| Schedule | Received | 2 Nov 2022  |
|          | Revised  | 30 May 2023 |
|          | Accepted | 6 Jun 2023  |

---

**Abstract** *Cupriavidus* sp. UYMMa02A is a beta-rhizobia strain of the *Cupriavidus* genus, isolated from nodules of *Mimosa magentea* in Uruguay. This strain can form effective nodules with several *Mimosa* species, including its original host. Genome analyses indicate that *Cupriavidus* sp. UYMMa02A has a highly conserved 35 kb symbiotic island containing *nod*, *nif*, and *fix* operons, suggesting conserved mechanisms for the symbiotic interaction with plant hosts. However, while *Cupriavidus* sp. UYMMa02A produces functional nodules and promotes *Mimosa pudica* growth under nitrogen-limiting conditions, *nod* genes are not induced by luteolin or exposure to *Mimosa* spp. root exudate. To explore alternative mechanisms implicated in the *Cupriavidus*-*Mimosa* interaction, we assessed the proteomic profiles of *Cupriavidus* sp. UYMMa02A grown in the presence of pure flavonoids and co-culture with *Mimosa pudica* plants. This approach allowed us to identify 24 differentially expressed proteins potentially involved in bacterial-plant interaction. In light of the obtained results, a possible model for *nod*-alternative symbiotic interaction is proposed.

---

**Keywords** (separated by '-')

Beta-rhizobia - *Cupriavidus* - Luteolin - Apigenin - Proteomic - 2D-DIGE - *Mimosa pudica* - *Mimosa magentea* - Root exudates

---

**Footnote Information** Cecilia Rodríguez-Esperón and Laura Sandes contributed equally to the present work.

---



# Nodulation in the absence of *nod* genes induction: alternative mechanisms involved in the symbiotic interaction between *Cupriavidus* sp. UYMMa02A and *Mimosa pudica*

Cecilia Rodríguez-Esperón<sup>1</sup> · Laura Sandes<sup>1</sup> · Ignacio Eastman<sup>1</sup> · Carolina Croci<sup>1,2</sup> · Florencia Garabato<sup>1</sup> · Virginia Ferreira<sup>1</sup> · Martín Baraibar<sup>3</sup> · Magdalena Portela<sup>4,5</sup> · Rosario Durán<sup>4</sup> · Raúl A. Platero<sup>1</sup>

Received: 2 November 2022 / Revised: 30 May 2023 / Accepted: 6 June 2023  
© The Author(s) under exclusive licence to Society for Environmental Sustainability 2023

## Abstract

*Cupriavidus* sp. UYMMa02A is a beta-rhizobia strain of the *Cupriavidus* genus, isolated from nodules of *Mimosa magentea* in Uruguay. This strain can form effective nodules with several *Mimosa* species, including its original host. Genome analyses indicate that *Cupriavidus* sp. UYMMa02A has a highly conserved 35 kb symbiotic island containing *nod*, *nif*, and *fix* operons, suggesting conserved mechanisms for the symbiotic interaction with plant hosts. However, while *Cupriavidus* sp. UYMMa02A produces functional nodules and promotes *Mimosa pudica* growth under nitrogen-limiting conditions, *nod* genes are not induced by luteolin or exposure to *Mimosa* spp. root exudate. To explore alternative mechanisms implicated in the *Cupriavidus*-*Mimosa* interaction, we assessed the proteomic profiles of *Cupriavidus* sp. UYMMa02A grown in the presence of pure flavonoids and co-culture with *Mimosa pudica* plants. This approach allowed us to identify 24 differentially expressed proteins potentially involved in bacterial-plant interaction. In light of the obtained results, a possible model for *nod*-alternative symbiotic interaction is proposed.

**Keywords** Beta-rhizobia · *Cupriavidus* · Luteolin · Apigenin · Proteomic · 2D-DIGE · *Mimosa pudica* · *Mimosa magentea* · Root exudates

## Introduction

Rhizobia are soil bacteria that engage in symbiotic interactions with legume plants. During this interaction, new specialized organs called nodules are formed in the roots (and sometimes in stems) of host plants. Inside the nodules, bacteria convert atmospheric nitrogen into ammonia in a process known as Symbiotic Nitrogen Fixation (SNF) (Lindström and Mousavi 2020).

The ability to form nitrogen-fixing nodules in symbiosis with legumes is restricted to alpha and beta subgroups of proteobacteria (Andrews and Andrews 2017). The best-characterized rhizobia species; *Sinorhizobium meliloti*, *Rhizobium leguminosarum*, or *Bradyrhizobium japonicum*, belong to the *Rhizobiaceae* family of alpha-proteobacteria. In beta-proteobacteria, the *Burkholderiaceae* family is the best characterized and includes just three genera *Paraburkholderia*, *Trinickia*, and *Cupriavidus* (Chen et al. 2001, 2003; Dall'Agnol et al. 2017; Estrada-de los Santos et al. 2018). Both *Paraburkholderia* and *Cupriavidus* rhizobia strains were described at the beginning of the twenty-first

Cecilia Rodríguez-Esperón and Laura Sandes contributed equally to the present work.

✉ Raúl A. Platero  
rplatero@iibce.edu.uy

<sup>1</sup> Laboratorio de Microbiología Ambiental, Departamento de Bioquímica y Genómica Microbianas, Instituto de Investigaciones Biológicas Clemente Estable, Ministerio de Educación y Cultura, Montevideo, Uruguay

<sup>2</sup> Present Address: Laboratorio de Ecología Microbiana Acuática, Departamento de Microbiología, Instituto de Investigaciones Biológicas Clemente Estable, Ministerio de Educación y Cultura, Montevideo, Uruguay

<sup>3</sup> OXIProteomics, Créteil, France

<sup>4</sup> Unidad Mixta de Bioquímica y Proteómica Analíticas, Institut Pasteur de Montevideo-Instituto de Investigaciones Biológicas Clemente Estable, Ministerio de Educación y Cultura, Montevideo, Uruguay

<sup>5</sup> Facultad de Ciencias, Universidad de la República, Montevideo, Uruguay

century. Since then, beta-rhizobia have been described as legume symbionts in America (Bontemps et al. 2010; Andam et al. 2007; dos Reis et al. 2010; Taulé et al. 2012), Africa (Garau et al. 2009; Howieson et al. 2013; Lemaire et al. 2015), Asia (Liu et al. 2012; Gehlot et al. 2013) and Oceania (Parker et al. 2007), primarily associated with legumes of Mimosoid clade, but also with some members of the *Papilionoideae* (Garau et al. 2009; Lemaire et al. 2015). Despite their worldwide distribution, the molecular mechanisms involved in the interaction between beta-rhizobia and host plants have been analyzed in a few model strains (Amadou et al. 2008; de Campos et al. 2017; Lardi et al. 2017; Klonowska et al. 2018; Bellés-Sancho et al. 2022; Rodríguez-Esperón et al. 2022). Genome analyses of beta-rhizobia that nodulate Mimosoid clade have shown the presence of a highly conserved and compact genomic region, known as the symbiotic island, that encodes for *nod*, *nif*, and *fix* genes (De Meyer et al. 2016; Zheng et al. 2017). The *nod* genes code for proteins involved in the synthesis (*nodBCHASUQ*) and exportation (*nodIJ*) of nodulation (Nod) factors, as well as their regulation (*nodD*). In turn, the *nif* genes encode proteins related to the nitrogenase complex (*nifH*, *nifD*, and *nifK*), regulation (*nifA*), and maturation processes (*nifEDXQ*). The *fix* genes encode membrane proteins required for electron transfer to generate the energy required for the SNF process (*fixABCX*; *fixNOPQ*).

In beta-rhizobia, *nod* genes are induced in the presence of pure flavonoids such as luteolin and apigenin (Marchetti et al. 2011; Rodríguez-Esperón et al. 2022) or root exudates of the host plant *Mimosa pudica* (Klonowska et al. 2018). In line with the conservation of this important recognition mechanism, other genes and molecules involved in bacteria-plant interaction have been identified in beta-rhizobia. These include the type-III secretion system (Saad et al. 2012) and synthesis of branched-chain amino acids in *Cupriavidus taiwanensis* LMG19424 (Chen et al. 2012); type VI secretion system (de Campos et al. 2017; Lardi et al. 2017) and synthesis of exopolysaccharide (EPS) cepacian in *Paraburkholderia phymatum* STM815 (Liu et al. 2020). Despite these few examples, there is still a lack of knowledge about the molecular mechanisms implicated in the symbiotic interaction between beta-rhizobia and legume hosts.

In Uruguay, beta-rhizobia have been identified as the main symbionts of *Parapiptadenia rigida* (Taulé et al. 2012) and *Mimosa* spp. (Platero et al. 2016; Pereira-Gómez et al. 2020). Phylogenetic analyses indicated that *Cupriavidus* strains symbiotically associated with these plants do not belong to the well-studied *C. taiwanensis* species but rather to the *C. necator* and other *Cupriavidus* species.

*Cupriavidus* sp. UYMMa02A was isolated from nodules of *Mimosa magentea*, a native legume found in the southeast region of Uruguay. Through a Multi-Locus Sequence Analysis (MLSA) approach, it was demonstrated

that UYMMa02A does not belong to the previously described *C. taiwanensis* and *C. necator*, but it may represent a novel rhizobial species within the *Cupriavidus* genus (Platero et al. 2016). Genome sequencing of *Cupriavidus* sp. UYMMa02A (Iriarte et al. 2016) indicated the presence of a conserved and compact symbiotic island that encodes for the *nod*, *nif*, and *fix* genes observed in other beta-rhizobia (Amadou et al. 2008; Moulin et al. 2014; De Meyer et al. 2015a, b, 2016). In addition, this strain induces pink nodules on the roots of its original host and other *Mimosa* species, including *M. pudica* (Platero et al. 2016).

The present study aimed to analyze the initial steps of the *Cupriavidus-Mimosa* symbiotic interaction. Firstly, we determined the expression of *nod* genes in *Cupriavidus* sp. UYMMa02A strain when cultivated in the presence of pure flavonoids or *Mimosa* spp. root exudates. Then we analyzed the proteomic changes induced in the bacteria by the presence of pure flavonoids and the plant host. Finally, we integrated the obtained results into a model that reports the changes occurring during the initial steps of the *Cupriavidus* sp. UYMMa02A—*Mimosa pudica* symbiotic interaction.

## Material and methods

### Bacterial strains, plasmids, and growth conditions

The bacteria and plasmids used in this study are listed in Table 1. *Escherichia coli* strains were grown aerobically at 37 °C in Luria–Bertani (LB) medium. *Cupriavidus* strains were grown at 30 °C in LB or M9 minimal medium containing 14 mM sodium citrate as a carbon source (Sambrook et al. 1989). When indicated M9 cultures were supplemented with 5 µM luteolin or apigenin. Modified M9 media containing *Mimosa* spp. root exudates were prepared to replace the original water volume used in M9, by filter-sterilized root exudates. When required the following antibiotics were used for strain selection; Ampicillin 100 µg ml<sup>-1</sup> (Ap), Nitrofurantoin 50 µg ml<sup>-1</sup> (Nf), Chloramphenicol 25 µg ml<sup>-1</sup> (Cf), and Tetracycline 8 µg ml<sup>-1</sup> (Tc).

### Sequence analysis

Homology searches and sequences retrieval were done via Internet server BLAST (NCBI, NIH, Bethesda, MD, USA: <http://www.ncbi.nlm.nih.gov>) and RAST server (Aziz et al. 2008). Sequence alignments were done by Mega v7.0.26 (Kumar et al. 2016) and SnapGene® software (from Insightful Science; available at [snapgene.com](http://snapgene.com)) was used for graphic presentation.

**Table 1** Strains and plasmids used in this work

| Strain   | Relevant characteristics   | Reference               |
|--|--|-------------------------|
| <i>Escherichia coli</i> DH5 $\alpha$                 | Cloning host; F <sup>-</sup> $\lambda^{-}$ <i>endA1 glnX44(AS) thiE1 recA1 relA1 spoT1 gyrA96(Nal<sup>R</sup>) rfbC1 deoR nupG <math>\Phi</math>80(lacZ<math>\Delta</math>M15) <math>\Delta</math>(argF-lac)169 hsdR17</i> | Hanahan (1983)          |
| <i>Cupriavidus</i> sp. UYMMa02A                      | Wild-type strain, isolated from <i>Mimosa magentea</i> nodules in Uruguay  | Platero et al. (2016)   |
| <i>Cupriavidus taiwanensis</i> LMG19424 <sup>T</sup> | Type strain. Isolated from <i>Mimosa pigra</i> nodules in Taiwan   | Chen et al. (2001)      |
| <i>Cupriavidus necator</i> UYPR2.512                 | Wild-type strain, isolated from <i>Parapiptadenia rigida</i> nodules in Uruguay  | Taulé et al. (2012)     |
| Plasmid  |  |                         |
| pRK600   | Helper plasmid used for conjugation, Cf <sup>R</sup>   | Kessler et al. (1992)   |
| pCZ388   | pLAFR6 derivative containing a promoterless <i>lacZ</i> gene, Tc <sup>R</sup>  | Cunnac et al. (2004)    |
| pCBM01   | pCZ388 containing 401 bp of the <i>Cupriavidus taiwanensis</i> LMG19424 <i>nodB</i> promoter, Tc <sup>R</sup>  | Marchetti et al. (2010) |

## 140 Reporter strains construction

141 To evaluate the expression of *nodB* gene promoter, plasmid  
 142 pCBM01 containing the *pnodB*<sub>19424</sub>-*lacZ* transcriptional  
 143 fusion (Marchetti et al. 2010) or plasmid pCZ388 containing  
 144 a promoterless *lacZ* (Cunnac et al. 2004) were introduced in  
 145 *Cupriavidus* spp. strains by triparental mating as previously  
 146 described (Rodríguez-Esperón et al. 2022).

## 147 Assessment of *pnodB*<sub>19424</sub>-*lacZ* gene expression

148 Cultures of *Cupriavidus* spp. strains carrying the plasmids  
 149 pCBM01 or pCZ388 were grown overnight at 30 °C using a  
 150 rotary shaker at 200 rpm, in 5 mL of M9 supplemented with  
 151 Tc. At the end of this time, a 1/100 (v/v) dilution was made  
 152 in fresh medium supplemented with 5  $\mu$ M luteolin ( $\geq$  98%  
 153 TLC, SIGMA, USA) or in a modified M9 prepared with  
 154 roots exudates and incubated for 18 h at 30°C. Uninduced  
 155 control cultures were included for each assay. Beta-galac-  
 156 tosidadase assays were performed according to the standard  
 157 Miller assay (Miller 1972).

## 158 Pre-treatment, surface sterilization, 159 and germination of *Mimosa* spp. seeds

160 *M. pudica* seeds were obtained commercially from Outside-  
 161 pride Seeds, LLC (Oregon, USA). *M. magentea* seeds were  
 162 collected from native plant populations growing in Uruguay  
 163 (Platero et al. 2016). The seeds were submerged in ethanol  
 164 95% for 2 min and dried in filter paper. After they were  
 165 treated with 10 M sulfuric acid for 20 min, followed by seven  
 166 washes with sterile distilled water. Finally, the seeds were  
 167 treated with 4% sodium hypochlorite for 5 min followed by  
 168 seven washes with sterile distilled water. Surface-sterilized  
 169 seeds were germinated on 0.8% (wt/vol) agar-water plates,  
 170 at 30 °C in dark conditions for 2 days.

## Roots exudate collection method

171 *Mimosa* spp. pre-germinated seeds were sown in a 250 mL  
 172 test glass jar (20 seeds per flask) containing 20 mL of sterile  
 173 water and a stainless-steel grate for seedling support. Plants  
 174 were incubated for five days under a photoperiod of 16 h  
 175 light/8 h darkness at 26 °C. After that, the water solution  
 176 containing the roots exudates was collected in 50 mL plastic  
 177 conical tubes, centrifuged for 5 min at 6,000 g to remove  
 178 cellular debris and supernatants were filtered-sterilized  
 179 using 0.45  $\mu$ m membrane filters (Millipore, USA). Filter-  
 180 sterilized root exudates were used, instead of water, for pre-  
 181 paring modified M9 media. All experiments including root  
 182 exudates were performed with freshly (same day) prepared  
 183 root exudates.  
 184

## Gene expression based on quantitative reverse transcription-PCR (RT-qPCR)

185 The RT-qPCR experiments were performed with *Cupriavi-*  
 186 *didus* sp. UYMMa02A growing in M9 with *M. pudica* root  
 187 exudates or M9 media. For the bacterial RNA extraction,  
 188 *Cupriavidus* sp. UYMMa02A was cultivated in 150 mL  
 189 of modified M9 with *M. pudica* root exudates or M9  
 190 until reaching the mid-exponential phase (OD<sub>600</sub> between  
 191 0.6–0.8). Cultures were then incubated for 20 min with  
 192 100  $\mu$ g/mL chloramphenicol and then rapidly cooled by  
 193 placing the tubes in a water–ice bath. Cells were recov-  
 194 ered by centrifuging at 5000g for 5 min at 4 °C. Obtained  
 195 pellets were suspended in 1.5 mL of lysis buffer (20 mM  
 196 Tris–HCl Buffer pH 7.6; 50 mM MgCl<sub>2</sub>; 150 mM NH<sub>4</sub>Cl  
 197 and transferred to 2 mL lysis tubes (MP Biomedicals Lysing  
 198 Matrix Tubes # Matrix B). Cell lysis was carried out on Fast  
 199 Prep equipment (MP Biomedicals) using a cycle of 6.0 m/s  
 200 for 60 s. Finally, lysates were centrifuged at 10,000g for  
 201 20 min at 4 °C, and supernatants containing the cell extract  
 202 were transferred to a new tube. One hundred microliters of  
 203 the obtained extracts were used for total RNA extraction  
 204  
 205

206 using a PureLink RNA Mini Kit (Thermo Fisher Scientific #12183018A). Obtained RNA was treated with 5 units  
 207 of DNase I (Thermo Fisher Scientific EN0521) for 5 min  
 208 at 37 °C. One microgram of total RNA was converted to  
 209 cDNA using the High-Capacity cDNA Reverse Transcription  
 210 Kit (Applied Biosystem), following the manufacturer's  
 211 recommendations. Quantitative PCR (qPCR) analyses were  
 212 performed essentially as described (Rodríguez-Esperón  
 213 et al. 2022). The UYMMa02A *efg* gene (ODV42482.1)  
 214 which encodes for the elongation factor G and the *s14* gene  
 215 (ODV43065.1) which encodes for the ribosome protein  
 216 S14, were used as reference genes. The UYMMa02A *nodA*,  
 217 *nodB*, and *nodC* genes were selected to analyze relative  
 218 gene expression. Primer Blast software was used to design  
 219 primer sets for *nodA*, *nodB*, *nodC*, *efg*, and *s14*. The fol-  
 220 lowing primers were used: *efg*-for (5'-GCGATCATTTGG  
 221 GACGAAGC-3'); *efg*-rev (5'-CGGACTCGACCATCTTCT  
 222 CG-3'); *s14*-for (5'-CTGTTCTACGTGTCAG-3'); *s14*-rev  
 223 (5'-TGATGTTGATGCGGTGTTTC-3'); *nodA*-for (5'-ACG  
 224 TCCTCGCTGTGATTCTG-3'); *nodA*-rev (5'-AGGTCC  
 225 GTTGCGTTCGATAG-3'); *nodB*-for (5'-TGGGGCAAT  
 226 TTCAGCTTCCA-3'); *nodB*-rev (5'-AGCGACTTCGTG  
 227 TCCTTCAG-3'); *nodC*-for (5'-CAGAGCTTGCCTCACTT  
 228 CA-3'); *nodC*-rev (5'-TGCATCGTCTCATAGTCGC-3').  
 229 qPCRs were performed on a C1000 Touch Thermal Cycler  
 230 (Bio-Rad) using the iQTM SYBR Green Supermix (Bio-  
 231 Rad). qPCRs conditions were as follows: 5 min at 95 °C,  
 232 40 cycles of 15 s at 95°C, 30 s at 60 °C and 30 s at 72 °C.  
 233 Primer specificity and dimer formation were checked by dis-  
 234 sociation curves. A mixture of cDNA from induced and non-  
 235 induced samples was used for calculating primer efficiency.  
 236 The relative gene expression level was calculated using the  
 237  $2^{-\Delta\Delta C_q}$  method, statistical analyses were performed in the  
 238 InfoStat statistical program (<https://www.infostat.com.ar/>).  
 239 Normal distribution of data was confirmed using the Sha-  
 240 piro–Wilk test and one-way ANOVA was used for sample  
 241 comparisons. Differences were considered statistically sig-  
 242 nificant if the p-value < 0.05.  
 243

#### 244 **Assessment of growth promotion capacity**

245 Germinated seeds prepared as described above were trans-  
 246 ferred into glass tubes containing 15 mL of Jensen's N-free  
 247 medium (36) solidified with 0.8% (wt/vol) agar. Seedlings  
 248 were inoculated with 1 mL of a rhizobial suspension con-  
 249 taining  $1 \times 10^7$  cfu. One milliliter of sterile water was added  
 250 to negative controls. Plants were grown under a photo-  
 251 period of 16 h light/8 h darkness at 26 °C. The presence  
 252 and coloration of root nodules were evaluated periodically.  
 253 Three months after inoculation, plants were harvested, and  
 254 plant height was measured and used as a proxy for the plant  
 255 growth promotion capacity of inoculated strains. The experi-  
 256 ment was repeated three times with at least 10 plants per

condition. Differences were considered statistically different  
 if the p-value < 0.01 according to the t-test.

#### **Cupriavidus sp. UYMMa02A-Mimosa pudica co-culture assays**

261 A co-culture device was constructed allowing bacterial-  
 262 plant signal exchange, but avoiding physical contact between  
 263 both organisms (Fig. 9). Bacterial containers were assem-  
 264 bled using 10 cm dialysis membrane tubing pieces (D9652,  
 265 Sigma Aldrich). Membranes were washed with distillate  
 266 water and one of their ends was sealed with a double knot,  
 267 the other end was attached to a 10 cm silicone tubing and  
 268 sealed with a plastic seal. For a complete and tight seal,  
 269 a small glass tube was inserted inside the silicone tubing.  
 270 Bacterial container sterilization was achieved by gamma-  
 271 irradiation using a 21 kGy dose in the irradiation facilities  
 272 of the Uruguayan Technological Laboratory (LATU). Test  
 273 glass jars of 250 mL containing 50 mL of N-free Howieson  
 274 (Howieson et al. 1993) liquid media diluted 1/10 (v/v) and  
 275 polypropylene balls as seedling support, were autoclaved for  
 276 20 min at 121 °C. After cooling, the jars were opened in the  
 277 laminar flow hoods, and bacterial containers were aseptically  
 278 added, submerging the membrane in the media and the sili-  
 279 cone tubing facing the jar lids. A total of 50 M. *pudica* ger-  
 280 minated seeds were sown in each jar and incubated under a  
 281 photoperiod of 16 h light/8 h darkness. After 5 days, the bac-  
 282 terial containers were filled through the silicone tubing, with  
 283 5 mL of  $1 \times 10^8$  cfu mL<sup>-1</sup> of *Cupriavidus sp. UYMMa02A*,  
 284 and incubated for another five days under the same condi-  
 285 tions of temperature and photoperiod. As control treatments,  
 286 plant-free systems were used. In these cases, Howieson liq-  
 287 uid media was supplemented with 2 mM sodium citrate as a  
 288 carbon source and 2 mM ammonium chloride as a nitrogen  
 289 source, to allow bacterial survival. Cell suspensions were  
 290 carefully transferred from the membranes to clean and sterile  
 291 plastic tubes and centrifuged for 5 min at 6000g. Bacterial  
 292 pellets were used for total protein extraction. A minimum of  
 293 three biological replicates were performed for each sample.

#### **Total protein extraction and solubilization**

295 For protein extraction, bacterial pellets were washed three  
 296 times with 2 mL of phosphate-buffered saline (PBS) and  
 297 resuspended in 10% of the original culture volume in  
 298 PBS containing  $1 \times$  complete-EDTA-Free protease inhibitor  
 299 (Roche). Cell lysis was performed by sonication (7  
 300 cycles  $\times$  30 s) in continuous mode and at a relative power  
 301 of 4 alternated with 30 s of rest in an ice-water bath, using  
 302 an ultrasonic homogenizer (Cole-Parmer Instruments Co.).  
 303 Cell lysates were separated by centrifugation at 12,000g  
 304 for 15 min at 4 °C and the supernatant containing the total

soluble proteins was kept at  $-20^{\circ}\text{C}$ . At least three biological replicates were performed per sample.

### Protein quantification

Protein concentration was estimated by the Bradford method (Bradford 1976) using bovine serum albumin (BSA) for calibration curves. The quality of protein fractions was verified by SDS-PAGE (Laemmli 1970).

### Protein precipitation

Previous to two-dimensional (2D) electrophoresis, proteins were precipitated, washed, and concentrated, using the commercial kit “2-D Clean Up Kit” (GE Healthcare, Amersham Biosciences) according to the manufacturer's instructions. Finally, proteins were resuspended in a rehydration buffer (8 M urea, 2 M thiourea, 4% CHAPS, 40 mM DTT, 1.2% (v/v) IPG buffer) pH 8.5.

### Protein labelling

Thirty-five  $\mu\text{g}$  of total proteins from each condition were labeled using the Refraction-2D™ Labelling Kit (NH DyeAGNOSTICS GmbH, Germany), following the manufacturer's recommendations. The samples were normalized and labeled with the Cy3 dye ( $\lambda_{\text{ex}} = 532 \text{ nm}/\lambda_{\text{em}} = 580 \text{ nm}$ ) or Cy5 ( $\lambda_{\text{ex}} = 633 \text{ nm}/\lambda_{\text{em}} = 670 \text{ nm}$ ), while Cy2 dye ( $\lambda_{\text{ex}} = 488 \text{ nm}/\lambda_{\text{em}} = 520 \text{ nm}$ ) was used to label the internal standard which consists of a pooled sample comprising equal amounts (10  $\mu\text{g}$ ) of all samples to be compared.

### 2D-DIGE electrophoresis

The labeled samples were mixed in hydration buffer (8 M urea, 2 M thiourea, 2% (p/v) CHAPS, and 1.2% (v/v) IPG-buffer) and loaded on 24-cm Immobiline DryStrips previously hydrated in the same buffer (nonlinear pH range 3–10, GE Healthcare). Isoelectric focusing (IEF) was run using an IPGphor III apparatus (GE Healthcare). The voltage profile used was adapted to run overnight with the following voltage program: constant phase of 500 V/2 h, constant phase of 2000 V/2 h, a linear increase to 4000 V/2 h, a linear increase to 8000 V/2 h, and a constant final phase at 8000 V for 4 h. After that, the IPG strips were allowed to equilibrate for 10 min with mechanical agitation in 1 mL of equilibration buffer (6 M urea, 50 mM Tris-HCl, pH 8.6, 30% glycerol, 2% sodium dodecyl sulfate) containing 1% DDT for 10 min. Then, reactions were quenched by immersing the strips in SDS-PAGE running buffer (25 mM Tris, 192 mM glycine, 0.1% SDS). As a second dimension, proteins were separated by SDS-PAGE gels (12% acrylamide-bisacrylamide) using an Ettan DALT-Six apparatus Electrophoresis System

electrophoresis cell maintained at  $20^{\circ}\text{C}$  with the Multitemp III cooling unit (GE Healthcare). Each strip was placed on the corresponding acrylamide gel and bound to it, using a running buffer containing 0.2% agarose and 0.002% (w/v) bromophenol blue. The runs were carried out at 100 mA and 80 V for the first 5 min and then the voltage was increased to 120 V until the run front reached the end of the gel.

### Image analysis

After 2D-DIGE electrophoresis, gels were fixed with ethanol:acetic acid: $\text{H}_2\text{O}$  (5:1:4) solution for 30 min. They were then scanned using a Typhoon 9500 FLA scanner (GE Healthcare), using the parameters recommended by the manufacturer, and analyzed using ImageQuant TL v8.1 software (GE Healthcare). The SameSpots software (TotalLab, Newcastle, UK) was used to match and analyze protein spots, allowing the detection, normalization with the internal standard, and quantification of the spots. Differential-in-gel analysis was used to calculate protein abundance alterations between samples on the same gel. The resulting spot maps for each biological replicate were then analyzed through biological variation analysis to provide statistical data on the differential protein expression. Spots that exhibited differences in the level of fluorescence with a p-value  $\leq 0.05$  and a rate of change  $\geq 1.25$  were considered as differentially regulated and selected for identification.

### Spot picking, protein digestion, and MALDI-TOF/TOF protein identification

To identify the differentially expressed proteins, gels were stained using Coomassie Brilliant Blue G-250 (Bio-Rad, Hercules, CA). Spots presenting significant differences were excised from gels, unstained with a solution of 0.1 M  $\text{NH}_4\text{HCO}_3$  in acetonitrile (ACN) 50% (v/v) and in-gel digested overnight using modified sequencing grade trypsin (Promega, Madison, USA). Peptide extraction was performed as previously described (Gil et al. 2019) and samples were desalted using Zip-Tip C18 reverse phase microcolumns (Millipore, Merck, USA) eluted directly on the plate using matrix solution ( $\alpha$ -cyano-4-hydroxycinnamic acid in 60% ACN, 0.1% TFA). The mixture was spotted onto an Opti-TOF plate of 384 positions (Ab Sciex). Spectra acquisition was performed on a MALDI-TOF/TOF MS (4800 Analyzer Abi Sciex) operated in positive reflector mode. The collected MS and MS/MS spectra of selected ions were externally calibrated using a standard peptide mix (Applied Biosystems). Protein identification was carried out using Mascot (Matrix Science, London, UK, (<http://www.matrixscience.com>)) in Sequence query mode, using the genome of *Cupriavidus* sp. UYMMa02A (GCA\_001725945.1) or the NCBI NR databases. The



399 search parameters were: Unrestricted taxonomy; allowable  
400 trypsin cleavage jumps = 1; partial modifications: oxidation  
401 of methionine and alkylation of cysteine by carbami-  
402 domethylation; peptide mass tolerance = 0.05 Da and MS/  
403 MS tolerance = 0.45 Da. For protein identification at least  
404 one MS/MS spectra per protein was required (with a Mascot  
405 peptide ion score  $p < 0.05$ ) and a  $p$ -value  $p < 0.05$  in the  
406 Mascot protein score. Proteins were classified into COGs  
407 functional categories and assigned to KEGG pathways  
408 using eggNOG-mapper (Huerta-Cepas et al. 2016) and also  
409 classified according to their subcellular location with the  
410 CELLO v.2.5 (Cheng et al. 2014). The genomic context of  
411 the proteins and the location of their gene sequence at the  
412 chromosomal level were analyzed by blast searches against  
413 the *Cupriavidus* sp. UYMMa02A genome annotated in the  
414 RAST server (Aziz et al. 2008).

## 415 Results

### 416 The genome of *Cupriavidus* sp. UYMMa02A encodes 417 a highly conserved symbiotic island

418 The draft genome of *Cupriavidus* sp. UYMMa02A was  
419 published in 2016 (Iriarte et al. 2016). Genome comparison  
420 among beta-rhizobial strains revealed a high level of synteny  
421 and nucleotide identity in operons containing the *nod*, *nif*,  
422 and *fix* genes (Fig. 1). However, there were differences in  
423 non-symbiotic and transposon-related genes within the sym-  
424 biotic islands leading to length heterogeneity among them.

The symbiotic island of *Cupriavidus* sp. UYMMa02A was  
425 the shortest with a predicted length of 33,908 bp. 426

427 A closer inspection of the *nod* operon in *Cupriavidus* sp.  
428 UYMMa02A indicated that eight *nod* genes, involved in Nod  
429 factors biosynthesis and exportation, namely *nodBCIJAH-*  
430 *SUQ*, are arranged in a single operon, while the *nodD* gene  
431 encoding a LysR-type transcriptional regulator, was located  
432 in the opposite orientation of *nodB* gene (Fig. 2). Moreover,  
433 a conserved NodD DNA binding motif known as nod-box  
434 (Schlaman et al. 1992) was identified in the intergenic region  
435 between *nodD* and *nodB* genes (Fig. 2). Minor differences  
436 in length and sequence were observed among the compared  
437 sequences, with the symbiotic islands of *Cupriavidus* sp.  
438 UYMMa02A and *Cupriavidus necator* UYPR2.512, showing  
439 the highest sequence homology.

### 440 The UYMMa02A *nod* operon is not induced by pure 441 flavonoids

442 The flavonoids luteolin and apigenin are known to induce  
443 the expression of *nod* genes in rhizobial *Cupriavidus* sp.  
444 strains (Amadou et al. 2008; Marchetti et al. 2010; Rod-  
445 ríguez-Esperón et al. 2022). The observed synteny lead us  
446 to hypothesize that the *nod* genes of *Cupriavidus* sp. UYM-  
447 Ma02A would be regulated by the same mechanism. To  
448 analyze this, *Cupriavidus* sp. UYMMa02A was transformed  
449 with the pCBM01 plasmid containing a *pnodB*<sub>19424</sub>-*lacZ*  
450 transcriptional fusion and beta-galactosidase (B-gal) activ-  
451 ity was compared with *C. necator* UYPR2.512 and *C. tai-*  
452 *wanensis* LMG19424, both harboring the same plasmid. As

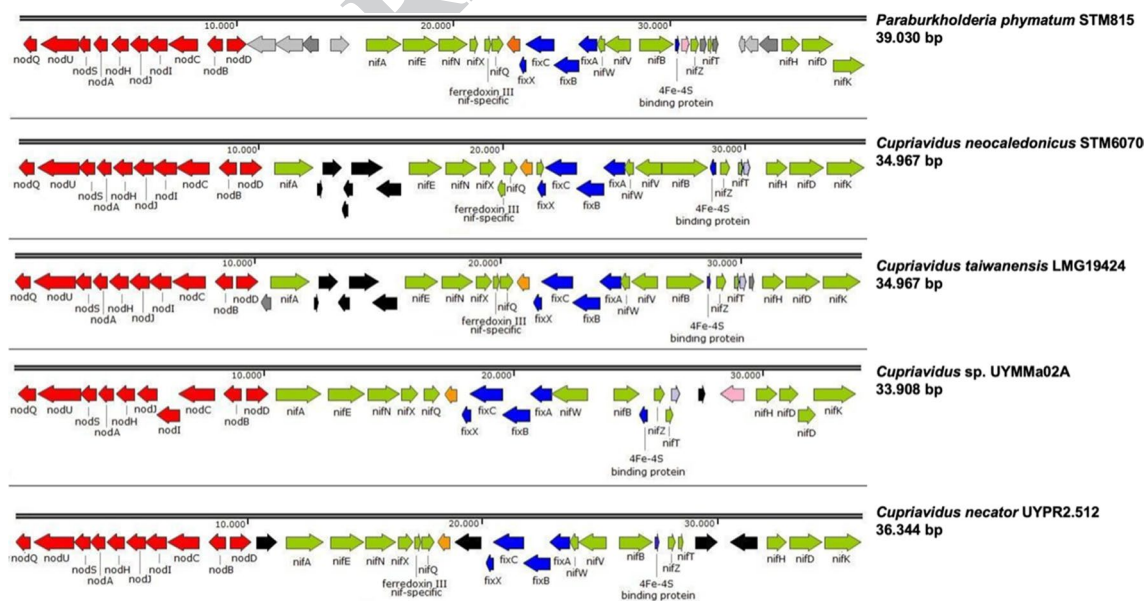


**Fig. 1** Comparison of symbiotic islands of different beta-rhizobia. The size of each symbiotic island is indicated below strain names. Genes belonging to the *nod/nif/fix* operons are coloured in red/green/

blue respectively, and transposons-related genes are coloured in black. Other colours represent genes that do not belong to the aforementioned operons

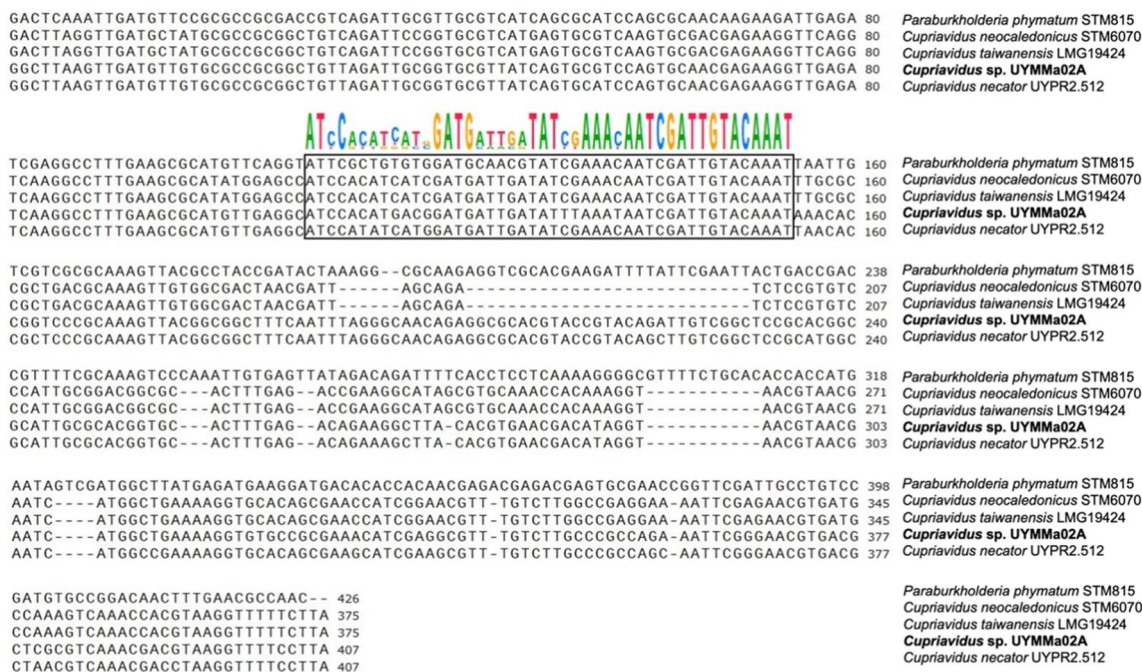


**Fig. 2** Sequence alignment of the *nodB-nodD* sequence in different Beta-rhizobia strains. Aligned sequences include the intergenic region between *nodB* and *nodD* and the first 100 bp of both genes. The black

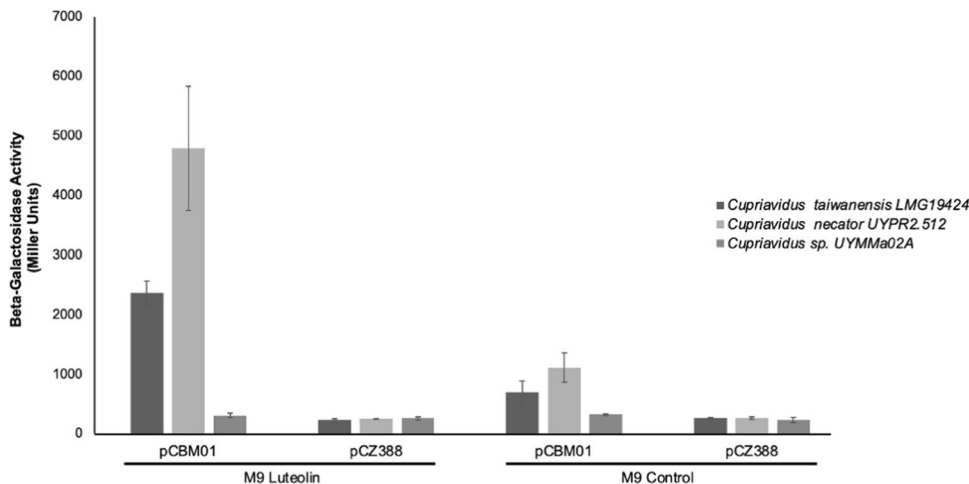
rectangle indicates *nod-box* localization. Conserved motifs are highlighted in colour letters

453 expected, a strong induction of B-gal activity was observed  
 454 for *C. necator* UYPR2.512 and *C. taiwanensis* LMG19424  
 455 in the presence of luteolin. However, *Cupriavidus* sp. UYM-  
 456 Ma02A remained unresponsive to the presence of pure fla-  
 457 vonoids (Fig. 3).

**Cupriavidus sp. UYMMa02A nod genes are not induced in the presence of Mimosa spp. root exudates**

458  
 459  
 460  
 461 Considering that *nod* genes expression is regulated by differ-  
 462 ent compounds in different rhizobial strains (Hungria et al.  
 463 1991; Schmidt et al. 1994; Jiménez-Guerrero et al. 2017), we  
 464 decided to investigate whether *Mimosa pudica* and *Mimosa*  
 465 *magentea* root exudates could serve as potential inducers  
 466 for *nod* genes expression in *Cupriavidus* sp. UYMMa02A.  
 467 Root exudates are complex solutions containing different

**Fig. 3** Expression of the *pnodB<sub>19424</sub>-lacZ* fusion in *Cupriavidus taiwanensis* LMG 19424, *Cupriavidus necator* UYPR2.512, and *Cupriavidus* sp. UYMMa02A in response to luteolin



468 amino acids, organic acids, sugars, and phenolic compounds,  
469 which have been shown to induce *nod* gene expression in *C.*  
470 *taiwanensis* LMG19424 (Klonowska et al. 2018).

471 A clear induction of *nod* gene expression was observed,  
472 as indicated by an increase in B-gal activity when *C. taiwan-*  
473 *ensis* LMG19424 and *C. necator* UYPR2.512 were grown  
474 in the presence of *Mimosa* spp. root exudates (Figs. 4 and  
475 5). These results indicate that *Mimosa pudica* and *Mimosa*  
476 *magentea* root exudates contain inducers for *nod* gene  
477 expression. However, when *Cupriavidus* sp. UYMMa02A  
478 was exposed to these root exudates, we did not observe  
479 any change in B-gal activity, suggesting that *nod* genes

480 expression was not induced in this strain (Figs. 4 and 5).  
481 Similar results were observed when pure flavonoids were  
482 used.

483 Altogether these findings suggest that the *pnodB*<sub>19424</sub>-*lacZ*  
484 is not responsive in *Cupriavidus* sp. UYMMa02A. However,  
485 we cannot exclude the possibility that endogenous *nod* genes  
486 in *Cupriavidus* sp. UYMMa02A *nod* genes could be induced  
487 but were not detected by the assay used. To directly assess  
488 this, we analyzed the mRNA levels of *nodA*, *nodB*, and *nodC*  
489 in *Cupriavidus* sp. UYMMa02A in the presence or absence  
490 of *M. pudica* root exudates (Fig. 6). No changes in the rela-  
491 tive *nod* gene expression were observed when *Cupriavidus*

**Fig. 4** Expression of the *pnodB*<sub>19424</sub>-*lacZ* fusion in *Cupriavidus taiwanensis* LMG19424, *Cupriavidus necator* UYPR2.512, and *Cupriavidus* sp. UYMMa02A in response to *Mimosa pudica* root exudates (RE)

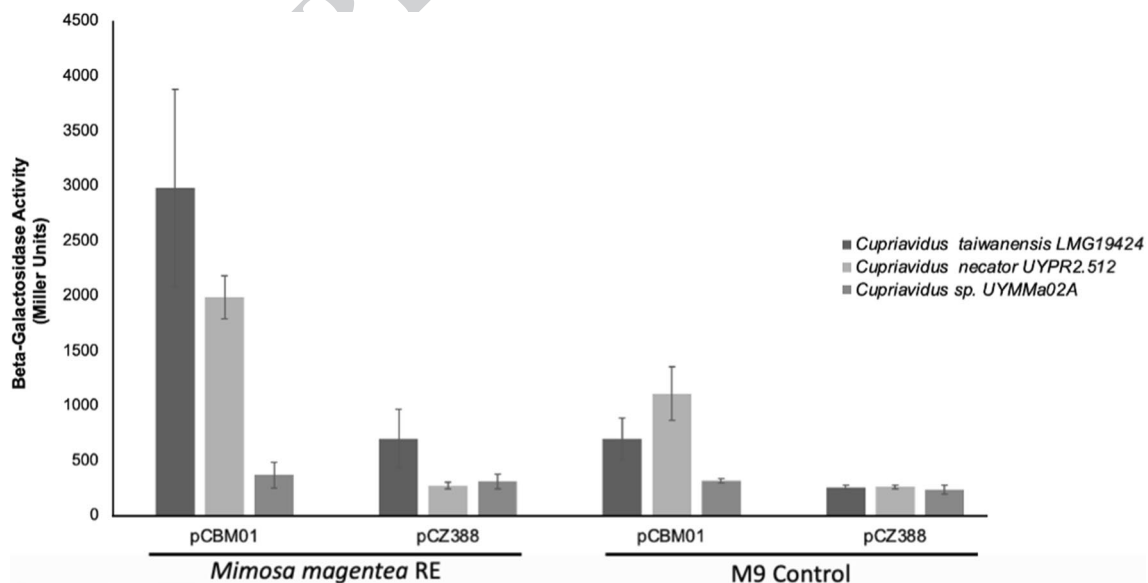
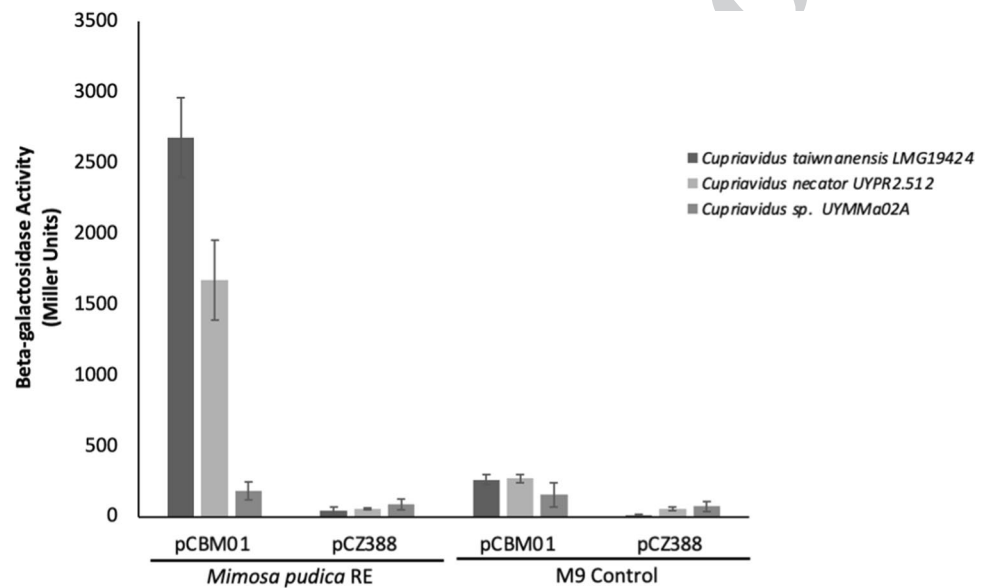
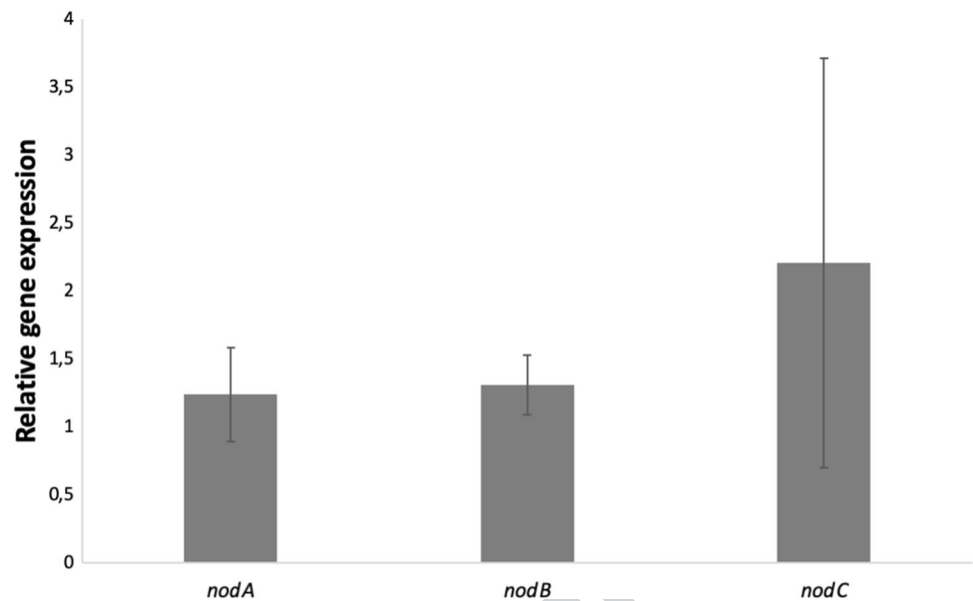


**Fig. 5** Expression of the *pnodB*<sub>19424</sub>-*lacZ* fusion in *Cupriavidus taiwanensis* LMG19424, *Cupriavidus necator* UYPR2.512, and *Cupriavidus* sp. UYMMa02A in response to *Mimosa magentea* root exudates (RE)

**Fig. 6** UYMMa02A *nodA*, *nodB*, and *nodC* expression in response to *M. pudica* root exudates. The bars represent the relative expression (Fold Change) of the *nodA*, *nodB*, and *nodC* genes to the housekeeping genes *elongation factor G (efg)* and *ribosomal protein S14 (S14)* when growing in M9 media supplemented with *M. pudica* root exudates versus in M9 media without exudates



492 sp. UYMMa02A was grown in the presence of *M. pudica*  
 493 root exudates compared to growth in M9 minimal media.  
 494 These results confirm the absence of *nod* genes induction in  
 495 *Cupriavidus* sp. UYMMa02A.

#### 496 ***Cupriavidus* sp. UYMMa02A induces functional 497 nodules and promotes *M. pudica* plant growth 498 in nitrogen-limiting conditions**

499 We have previously shown that *Cupriavidus* sp. UYM-  
 500 Ma02A can form nodules in the roots of several *Mimosa*  
 501 sp. including *M. pudica* plants (Platero et al. 2016). How-  
 502 ever, there was no direct evidence of this symbiotic inter-  
 503 action's plant growth promotion ability. When *M. pudica*  
 504 plants growing in nitrogen-free media were inoculated with  
 505 *Cupriavidus* sp. UYMMa02A, we observed the formation  
 506 of reddish nodules in the roots and a significant increase in  
 507 plant height (Fig. 7), strongly supporting the proficiency of  
 508 this symbiotic pair.

#### 509 **Proteomic changes induced by luteolin 510 and apigenin in *Cupriavidus* sp. UYMMa02A**

511 The lack of induction of *nod* genes suggests that alterna-  
 512 tive mechanisms could be involved in the establishment  
 513 of the *Cupriavidus* sp. UYMMa02A-*M. pudica* symbiotic  
 514 interaction. To determine the significance of this finding,  
 515 we decided to employ a proteomic approach known as Dif-  
 516 ferential In Gel Expression (DIGE) (Meleady 2018; Moze-  
 517 jko-Ciesielska and Mostek 2019). In the first approach,  
 518 bacteria were grown in the presence of luteolin or apigenin,  
 519 and total protein profiles were compared with bacteria  
 520 growing in the absence of the flavonoids. Two-dimensional

electrophoresis allowed us to separate 373 different spots, 521  
 representing around 4.5% of the CDS encoded by *Cupri-* 522  
*avidus* sp. UYMMa02A genome (Iriarte et al. 2016). DIGE 523  
 analysis showed 17 spots with altered expression levels in 524  
 the presence of luteolin while 16 spots were differentially 525  
 expressed in the presence of apigenin. When we performed 526  
 a combined analysis of differentially expressed spots in the 527  
 presence of the flavonoids versus the control condition, a 528  
 total of 22 differentially expressed spots were detected, 8 529  
 overrepresented in the luteolin condition, 8 in the apigenin 530  
 condition, and 6 in the control condition. After Coomassie 531  
 blue staining and gel excision, a total of 9 proteins were 532  
 identified by MALDI-TOF analyses (Table 2). According to 533  
 COG analyses, 3 of the identified proteins belong to Cat- 534  
 egory E (Amino acid transport and metabolism) and 3 to 535  
 category C (Energy conversion and production), one protein 536  
 to Category I (Lipids transport and metabolism), and one 537  
 belong to category P (inorganic ion transport). Except for the 538  
 tricarboxylate transporter protein TctC with a periplasmic 539  
 localization, all the identified proteins were predicted to be 540  
 cytoplasmic. A model summarizing the major findings using 541  
 this approach is shown in Fig. 8. 542

#### 543 **Differential protein expression during *Cupriavidus* 544 sp. UYMMa02A-*Mimosa pudica* co-cultures**

545 The next step in elucidating the mechanisms involved in  
 546 the plant-bacteria interaction was to determine the prot-  
 547 eomic responses of *Cupriavidus* sp. UYMMa02A to the  
 548 presence of plant host *Mimosa pudica*. We implemented a  
 549 co-culture device intended to allow plant-bacteria signal  
 550 interchange, preventing physical contact between sym-  
 551 biotics. In this device, plants were grown hydroponically

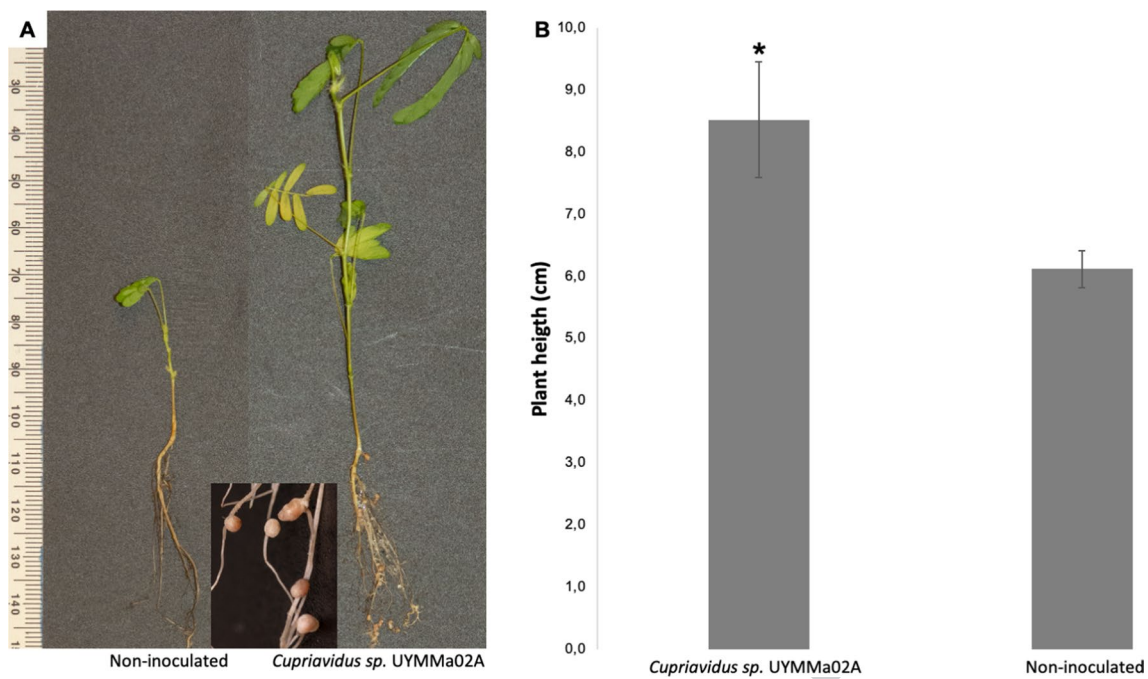


**Fig. 7** *Mimosa pudica* growth promotion ability of *Cupriavidus* sp. UYMMa02A. **A.** Examples of *M. pudica* development phenotype when inoculated with *Cupriavidus* sp. UYMMa02A or not inoculated. Insert, detail of the nodules formed by *Cupriavidus* sp. UYMMa02A in *M. pudica* roots. **B.** *M. pudica* plant height was recorded

30 days post-inoculation with *Cupriavidus* sp. UYMMa02A or with water as non-inoculated control. Asterisk indicates significant differences ( $p$ -value  $< 0.01$ ) between inoculated plants and non-inoculated plants

552 with bacteria placed in a closed dialysis membrane sub-  
 553 merged in the same hydroponic solution (Fig. 9). Protein  
 554 profile expression under co-culture conditions was compared  
 555 with bacterial cells cultivated in the same conditions,  
 556 but in that case, *Mimosa* plants were not included.  
 557 The hydroponic solution was supplemented with minimal  
 558 amounts of carbon and nitrogen sources to allow bacterial  
 559 survival. Image analyses of the 2D gels captured a total of  
 560 674 spots, representing around 8% of the bacterial encode  
 561 capacity. Thirty-seven differentially expressed spots were  
 562 determined (26 and 11 spots were overexpressed and  
 563 repressed respectively). After staining and excision from  
 564 the gels, 17 different proteins were identified by MALDI-  
 565 TOF, belonging to 11 different COG categories. Notably,  
 566 proteins categorized in the categories O (posttranslational  
 567 modifications and chaperones), G (carbohydrate transport  
 568 and metabolism), and M (membrane and cell wall) con-  
 569 tains both induced and repressed proteins, while proteins  
 570 in category T (transduction signals mechanisms) were  
 571 found overexpressed (Table 3). Subcellular localization  
 572 analysis identified 9 cytoplasmic proteins, 3 periplasmic  
 573 proteins, and 1 outer membrane protein, while 5 proteins  
 574 were predicted to be found both at the bacterial cytoplasm  
 575 and extracellularly. A model integrating the major findings  
 576 using this approach is presented in Fig. 10.

## Discussion

577  
 578 The presence of highly conserved symbiotic islands in the  
 579 genome of rhizobial *Cupriavidus* spp. suggest the exist-  
 580 ence of conserved symbiotic mechanisms among these  
 581 strains. Notwithstanding, gene expression analyses have  
 582 indicated that pure flavonoids or *Mimosa* spp. root exu-  
 583 dates are ineffective in inducing *Cupriavidus* sp. UYM-  
 584 Ma02A *nod* genes transcription. This is intriguing since  
 585 it has been shown that the presence of luteolin or apigenin  
 586 induces the synthesis and exportation of Nod factors in  
 587 *C. taiwanensis* LMG19424 (Amadou et al. 2008). In addi-  
 588 tion, these flavonoids were shown to induce the expression  
 589 of the *pnodB*<sub>19424</sub>-*lacZ* transcriptional fusion present in  
 590 pCBM01, in both *C. taiwanensis* LMG19424 (Marchetti  
 591 et al. 2010) and *C. necator* UYPR2.512 (Rodríguez-  
 592 Esperón et al. 2022). It is well known that the flavonoid  
 593 effect on *nod* genes regulation is dependent on the NodD  
 594 regulatory protein (Schlaman et al. 1992). Different NodD  
 595 proteins respond to different flavonoids, being this mecha-  
 596 nism one of the bases of the rhizobium-legume specificity  
 597 (Masson-Boivin et al. 2009). Small differences could be  
 598 observed at *Cupriavidus* sp. UYMMa02A NodD protein  
 599 sequence and in the *nodB*-*nodD* intergenic sequence in

**Table 2** *Cupriavidus* sp. UYMMa02A proteins differentially expressed in the presence of apigenin and luteolin

| Spot                               | Fold change | p value | Mascot score | Sequence coverage (%) | IP  | MW (kDa) | Identified protein  | ID             | COG category | Localization |
|------------------------------------|-------------|---------|--------------|-----------------------|-----|----------|---|----------------|--------------|--------------|
|                                    |             |         |              |                       |     |          |   |                |              |              |
| <b>Apigenin induced proteins</b>   |             |         |              |                       |     |          |   |                |              |              |
| 103                                | 1.5         | 0.019   | 163          | 18                    | 5.5 | 60.8     | Bifunctional aspartate transaminase/aspartate 4-decarboxylase   | WP_224080690.1 | E            | Cytoplasmic  |
| 272                                | 1.4         | 0.027   | 185          | 38                    | 5.8 | 27.9     | Enoyl-CoA hydratase   | ODV41316.1     | I            | Cytoplasmic  |
| 257                                | 1.5         | 0.004   | 157          | 16                    | 9.6 | 33.4     | Tripartite tricarboxylate transporter substrate binding protein | WP_011299555.1 | C            | Periplasmic  |
| 224                                | 1.5         | 0.052   | 157          | 33                    | 5.9 | 39.4     | Branched chain amino acid aminotransferase                      | ODV41908.1     | E            | Cytoplasmic  |
| <b>Luteolin induced proteins</b>   |             |         |              |                       |     |          |   |                |              |              |
| 103                                | 1.5         | 0.050   | 163          | 18                    | 6   | 60.8     | Bifunctional aspartate transaminase/aspartate 4-decarboxylase   | WP_224080690.1 | E            | Cytoplasmic  |
| 317                                | 1.4         | 0.021   | 94           | 44                    | 6   | 18.2     | DNA starvation/stationary phase protection protein              | WP_211952485.1 | P            | Cytoplasmic  |
| 335                                | 3.4         | 0.001   | 239          | 33                    | 6   | 55       | Aldehyde dehydrogenase  | ODV42183.1     | C            | Cytoplasmic  |
| <b>Apigenin repressed proteins</b> |             |         |              |                       |     |          |   |                |              |              |
| 155                                | 1.4         | 0.002   | 143          | 36                    | 9   | 32.1     | E2 component of the 2-oxoglutarate dehydrogenase complex        | WP_211945176.1 | C            | Cytoplasmic  |

comparison with *C. taiwanensis* LMG19424 and *C. necator* UYPR2.512. Thus, it is possible that *Cupriavidus* sp. UYMMa02A NodD protein does not become activated by the presence of flavonoids or this protein could not recognize the *C. taiwanensis* LMG19424 *nodB* promoter region present in the *pnodB*<sub>19424</sub>-*lacZ* used here. To overcome these limitations, we used *M. magentea* and *M. pudica* root exudates for *nod* genes expression analyses, however no changes in the expression levels of *nod* genes in *Cupriavidus* sp. UYMMa02A were observed. These results indicated that in *Cupriavidus* sp. UYMMa02A *nod* genes may not be involved in the first steps of the symbiotic interaction and suggest the existence of alternative mechanisms to Nod factors for bacterial-plant interaction. It is now known that some rhizobial strains are naturally able to engage in symbiotic interactions with their plant host in a Nod-factor-independent way. Researchers have discovered strains of *Bradyrhizobium* sp. lacking the canonical *nodABC* genes that can effectively nodulate *Aeschynomene* spp. (Giraud et al. 2007; Miché et al. 2010) and *Arachis hypogaea* (Guha et al. 2022).

The lack of induction of *nod* genes in *Cupriavidus* sp. UYMMa02A prompted us to search for alternative mechanisms involved in bacterial-plant interaction. To identify proteins potentially implicated in the initial steps of this process, we analyzed the patterns of protein expression of *Cupriavidus* sp. UYMMa02A when exposed to pure flavonoids and during plant co-culture conditions. The response to different *nod* gene-inducing flavonoids and root exudates derived from the plant host has been studied in various rhizobial species, mostly belonging to the alpha-proteobacteria class, using transcriptomic and proteomic approaches (Jiménez-Guerrero et al. 2017; diCenzo et al. 2019). These studies have demonstrated, that in addition to *nod* genes, flavonoids, and root exudates can influence the expression of several bacterial genes encoded by different bacterial replicons. When comparing the responses to flavonoids, and root exudates, there is only partial overlap, particularly in *nod*-related genes, indicating that specific mechanisms are regulated in response to distinct stimuli (Capela et al. 2005). In addition, these responses are often specific to the genus and strains of rhizobia (Fagorzi et al. 2021).

Only two works that used omics approaches have been published for the analysis of rhizobial *Cupriavidus* strains response to flavonoids (Rodríguez-Esperón et al. 2022) or host root exudates (Klonowska et al. 2018). Both works showed the differential expression of hundreds of genes, located at different bacterial replicons, in response to these stimuli. In agreement with this, upon luteolin and apigenin or co-culture conditions, *Cupriavidus* sp. UYMMa02A experiences significant changes at the proteomic level. Approximately 6% (22 out of 357 spots) of the *Cupriavidus* sp. UYMMa02A proteome changed in response to the presence

**Fig. 8** UYMMa02A proteins and pathways observed in response to flavonoids. Proteins differentially expressed in the presence of apigenin and/or luteolin are highlighted in bold. Green and red arrows indicate if proteins were found either upregulated (up direction) or downregulated (down direction), with respect to the control condition. The main cellular processes affected are indicated in bold and cursive text. See the text for a full description

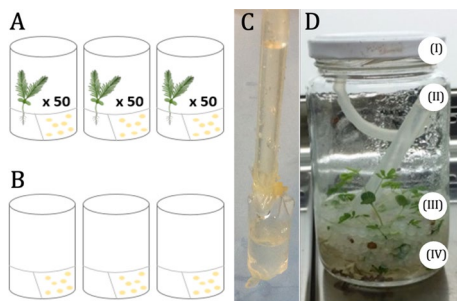
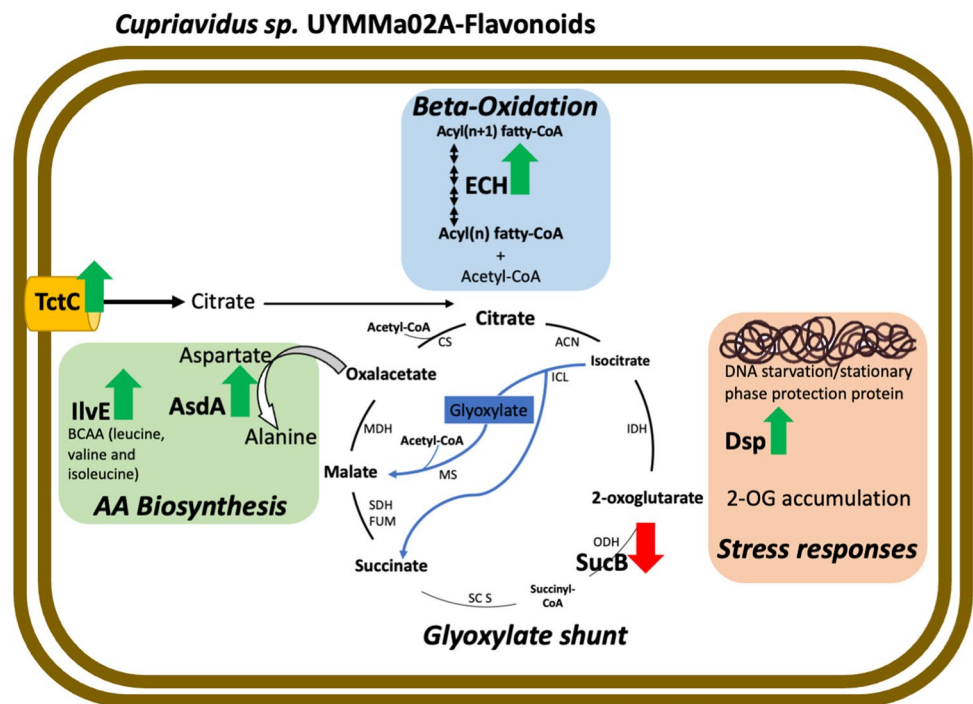


**Fig. 9** Plant-microorganism co-culture system. Bacteria were grown in the presence (A) or absence (B) of *M. pudica* plants. To prevent direct physical interaction between symbionts, the bacteria were placed inside a membrane tubing (C). D Picture of the real co-culture assembled system (I) jar lid; (II) silicone tube connected to the membrane for bacterial inoculation; (III) *M. pudica* plants; (IV) Mineral plant culture medium containing polypropylene balls for seedling support. As control treatments, plant-free systems were used (B)

of flavonoids, suggesting that these molecules are indeed signal molecules for this *Cupriavidus sp.* strain. In agreement with the observed lack of induction of the *pnodB*<sub>19424</sub>-*lacZ* transcriptional fusion, we did not detect the differential expression of proteins belonging to the symbiotic Island. Indeed, most of the affected proteins identified were related to the energy conversion and production (C) and amino acid metabolism (E) COG categories, indicating that flavonoids induce metabolic changes in *Cupriavidus sp. UYMMa02A*. The overexpression of the tricarboxylate transport protein (TctC) could reflect an increase in citrate transport, the only carbon source in the used media. Under these conditions,

citrate would be incorporated into the *Cupriavidus* metabolism directly through the citrate cycle (TCA or Krebs cycle), serving as an energy source and a carbon skeleton source. However, the concomitant diminution of the E2 component of the 2-oxoglutarate dehydrogenase complex would slow down the conversion of 2-oxo-glutarate (2-OG) to Succinyl-CoA. This change would result in the accumulation of 2-OG, a key biosynthetic intermediate that connects carbon and nitrogen metabolism. The 2-OG molecule is also involved in modulating enzyme activity and detoxifying reactive oxygen species (ROS) (Huego and Dixon 2015). Considering this, our result may indicate that some of the metabolic changes observed after exposure to luteolin and apigenin in *Cupriavidus sp. UYMMa02A* could be related to an oxidative stress response. In that sense, Mailloux and collaborators have shown that in response to oxidative stress, *Pseudomonas fluorescens* increased the activity of an NADP-dependent isocitrate dehydrogenase while decreasing the activity of the 2-oxoglutarate dehydrogenase complex, leading to the accumulation of 2-OG (Mailloux et al. 2007). Supporting this hypothesis, we also observed a rise in the DNA starvation/stationary phase protection protein (DpsA), which belongs to the ferritin superfamily and is involved in DNA binding and protection during starvation and/or oxidative stress conditions (Martinez and Kolter 1997; Gambino and Cappitelli 2016; Orban and Finkel 2022). Since luteolin and apigenin have been reported to scavenge ROS (Wu et al. 2015; Salehi et al. 2019; Caporali et al. 2022), it is unlikely that the flavonoids themselves are causing oxidative stress. Instead, the flavonoids may act as signals, advertising that

**Table 3** Proteins differentially expressed during *Cupriavidus* sp. and *Mimosa pudica* co-cultures

| Spot                      | Fold change | p value | Mascot score | Sequence coverage (%) | IP  | MW (KDa) | Identified protein  | COG category   |    | Localization              |
|---------------------------|-------------|---------|--------------|-----------------------|-----|----------|---|----------------|----|---------------------------|
|                           |             |         |              |                       |     |          |   | Protein name   | ID |                           |
| <b>Induced proteins</b>   |             |         |              |                       |     |          |   |                |    |                           |
| 507                       | 1.5         | 0.029   | 147          | 27                    | 6.1 | 15.3     | Nucleoside-diphosphate kinase Ndk                             | WP_211957553.1 | F  | Cytoplasmic/extracellular |
| 629                       | 1.8         | 0.036   | 181          | 40                    | 9.3 | 32.1     | ABC transporter, substrate-binding protein XylF               | ODV42702.1     | G  | Extracellular/cytoplasmic |
| 292                       | 2.4         | 0.005   | 109          | 13                    | 9   | 42.2     | Outer membrane protein Porin                                  | WP_224081450.1 | M  | Outer membrane            |
| 308                       | 2.3         | 0.041   | 111          | 39                    | 5.2 | 36       | Acetoin dehydrogenase E1 component beta-subunit               | WP_220630611.1 | -  | Cytoplasmic               |
| 357                       | 1.2         | 0.026   | 348          | 28                    | 5.6 | 27.5     | enoyl-ACP reductase FabI                                      | WP_211945097.1 | I  | Cytoplasmic/periplasmic   |
| 391                       | 1.8         | 0.034   | 184          | 51                    | 6.2 | 24.1     | Peroxi-redoxin  | WP_211946599.1 | O  | Periplasmic               |
| 499                       | 1.5         | 0.035   | 74           | 12                    | 5.9 | 16.2     | RidA family protein   | WP_211958671.1 | J  | Cytoplasmic               |
| 462                       | 1.3         | 0.041   | 352          | 66                    | 5.7 | 18.1     | Cyclophilin/peptidylprolyl isomerase                          | ODV42271.1     | O  | Cytoplasmic               |
| 199                       | 1.5         | 0.004   | 251          | 37                    | 6.2 | 43.3     | Efflux RND periplasmic adaptor subunit                        | ODV41844.1     | P  | Periplasmic               |
| 361                       | 1.3         | 0.007   | 126          | 28                    | 7   | 27.6     | Enoyl-CoA hydratase   | ODV41316.1     | Q  | Cytoplasmic               |
| 528                       | 1.4         | 0.036   | 237          | 65                    | 6.3 | 15.2     | Universal stress protein UspA                                 | WP_071013637.1 | T  | Extracellular/cytoplasmic |
| 512                       | 1.3         | 0.002   | 156          | 18                    | 5.2 | 15.8     | Universal stress protein UspA                                 | ODV41046.1     | T  | Extracellular/cytoplasmic |
| 78                        | 1.7         | 0.013   | 216          | 52                    | 5.5 | 73.4     | Serine protein kinase PrkA                                    | ODV43245.1     | T  | Cytoplasmic               |
| 74                        | 1.7         | 0.027   | 130          | 19                    | 5.5 | 73.4     | Serine protein kinase PrkA                                    | ODV43245.1     | T  | Cytoplasmic               |
| <b>Repressed proteins</b> |             |         |              |                       |     |          |   |                |    |                           |
| 106                       | 1.3         | 0.03    | 163          | 18                    | 5.5 | 60.8     | Bifunctional aspartate transaminase/aspartate 4-decarboxylase | WP_011298857.1 | E  | Cytoplasmic               |
| 113                       | 2.7         | 0.01    | 221          | 37                    | 8.4 | 62.5     | PPQ-dependent dehydrogenase                                   | WP_224007080.1 | G  | Periplasmic               |
| 625                       | 1.4         | 0.047   | 459          | 42                    | 5.1 | 57.3     | Chaperonin GroEL  | WP_035877914.1 | O  | Cytoplasmic               |



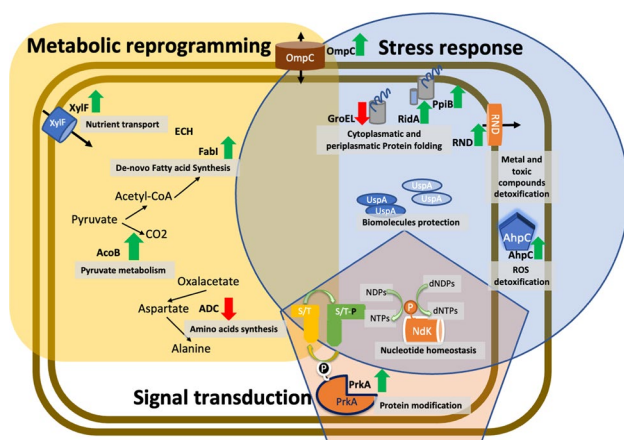


**Fig. 10** Model for the proteomics response of *Cupriavidus* sp. UYM-Ma02A-*Mimosa pudica* co-culture treatment. The illustration shows the main metabolic pathway, biological functions, chemical reactions, enzymes, and other proteins regulated in *Cupriavidus* sp. UYM-Ma02A grown in a co-culture system with the plant host *M. pudica*. Green and red arrows indicate proteins either upregulated (up direction) or downregulated (down direction) with respect to the control condition. Metabolic pathways affected are shadowed in grey. Color shadows were used to cluster affected proteins according to cellular processes; Metabolic reprogramming (in yellow), Stress response (in blue), and Signal transduction (in orange). Proteins implicated in more than one cellular process have been included at shadow intersections. See the text for a full description

oxidative could occur during the forthcoming interaction with plant roots, as the local production of ROS is a common feature observed during plant-bacteria interactions (Oldroyd et al. 2011; Gourion et al. 2015; Janczarek et al. 2015a, b).

The increased levels of the bifunctional enzyme Aspartate-Transaminase/Aspartate-4-decarboxylase (AsdA) and the Branched chain amino acids aminotransferase (IlvE) in the presence of luteolin and apigenin suggest that flavonoids impact amino acid metabolism in *Cupriavidus* sp. UYM-Ma02A. AsdA catalyzes the transamination of oxaloacetate to L-aspartate and the subsequent decarboxylation of aspartate to alanine (Kakimoto et al. 1969; Chen et al. 2000). The exportation of alanine and aspartate, through an amino acid cycle between bacteroids and plants, has been postulated to be important for SNF (Prell and Poole 2006; Prell et al. 2009). Besides this, the increase in the IlvE aminotransferase levels indicates the activation of branched-chain amino acids (BCAA) biosynthesis in response to flavonoids. BCAAs have been shown to have an essential role in the formation of effective symbiosis between the beta-rhizobia *Paraburkholderia phyantum* STM815, and *Cupriavidus taiwanensis* LMG19424 with *Mimosa pudica* plants (Chen et al. 2012). Furthermore, our recent findings have demonstrated that *C. necator* UYPR2.512 induces the expression of genes related to BCAAs transport in response to luteolin (Rodríguez-Esperón et al. 2022). Nonetheless, it should be considered

that the statistical support for ilvE protein is borderline, and further experiments will be needed to clarify its role as well as the role of BCAAs in the *Cupriavidus* sp. UYMMa02A-plant interaction.

A third process influenced by the presence of flavonoids in *Cupriavidus* sp. UYMMa02A is the possible activation of the glyoxylate cycle (Kornberg 1966). In this cycle, isocitrate is converted to succinate and glyoxylate by the enzyme isocitrate lyase (ICL) followed by the synthesis of malate from glyoxylate and acetyl-CoA by malate synthase (MS). The glyoxylate cycle enables growth using C<sub>2</sub> compounds by bypassing the CO<sub>2</sub>-generating steps of the TCA cycle while generating the necessary products for gluconeogenesis and other biosynthetic purposes (Dunn et al. 2009). Our hypothesis is supported by the following arguments: (a) The activation of this cycle would explain the observed drop in the levels of the E2 component of the 2-oxoglutarate dehydrogenase complex, as this enzyme is by-passed in the cycle (b) The glyoxylate cycle would fulfill the increased demand for 2-oxoglutarate, the substrate of the induced aspartate transaminase/aspartate 4-decarboxylase. Since each turn of the cycle needs two molecules of acetyl-CoA, the third piece of evidence supporting our proposal is the observed increase in the enoyl-CoA hydratase (ECH) levels. This enzyme catalyzes the second step in the beta-oxidation pathways of fatty acid metabolism (Moskowitz and Merrick 1969) and would supply the needed acetyl-CoA molecules to fuel the glyoxylate cycle. While some of the changes induced by the assayed flavonoids in *Cupriavidus* sp. UYMMa02A can be linked to metabolic processes implicated in the symbiotic interaction between rhizobia and host plants, additional experiments should be performed to determine the significance of these findings in interactions involving *Cupriavidus* rhizobial strains.

To improve the simulation of the initial steps of the symbiotic interaction between *Cupriavidus* sp. UYMMa02A and *Mimosa pudica*, we implement a co-culture device. Under these experimental conditions, we observed a broader bacterial response, as reflected by the number and distribution of proteins with altered expression among COG categories. Many of the proteins with changed expression were predicted to be located at periplasmic or extracellular space, suggesting that *Cupriavidus* sp. UYMMa02A undergoes changes at the membrane and periplasmic levels during the co-culture conditions. Surface remodeling has been well documented in many rhizobia models during their interaction with plant hosts. Variations in exopolysaccharides (EPS), lipopolysaccharides (LPS), and capsular polysaccharides (KPS) composition are required for the proper recognition of rhizobial cells by plant hosts, and for evading the natural plant immune system (Janczarek et al. 2015a, b). Under our experimental conditions, we observed the augmented expression of FabI, an enoyl-ACP reductase involved in

774 fatty-acid biosynthesis, which could reflect an upregulation  
 775 of lipogenesis for membrane remodeling. Membranes are  
 776 the primary barriers for cellular interaction with the environ-  
 777 ment, influencing the uptake and efflux of small molecules.  
 778 The observed increase in OmpC levels in *Cupriavidus* sp.  
 779 UYMMa02A during the co-culture could indicate the need  
 780 to enhance the transport of nutrients, signal molecules, or  
 781 other metabolites across the bacterial outer membrane. The  
 782 concomitant levels rise in the periplasmic binding compo-  
 783 nent of an ABC transport system (XylF) putatively involved  
 784 in ribose/xylose/arabinose/galactose acquisition, suggests  
 785 an enhanced transport capacity for these sugars. Xylose and  
 786 ribose have been detected in *M. pudica* root exudate (Klo-  
 787 nowska et al. 2018), implying that these sugars may support  
 788 *Cupriavidus* sp. UYMMa02A metabolism in the rhizosphere  
 789 of *M. pudica*. In the other hand, we also observed an increase  
 790 in the levels of a protein predicted to encode the periplas-  
 791 mic adaptor subunit of the resistance-nodule-division (RND)  
 792 family efflux transporter. In gram-negative bacteria, RND  
 793 efflux systems work in concert with outer membrane porins,  
 794 like OmpC, to detoxify deleterious compounds (Nies 2003;  
 795 Klonowska et al. 2020). The importance of RND systems  
 796 has been demonstrated in many rhizobial species, where  
 797 they play a crucial role in survival and competence in the  
 798 rhizosphere, affecting nodule formation and nitrogen fixa-  
 799 tion (Klonowska et al. 2012; Santos et al. 2014). Moreover,  
 800 as observed here, some of these systems were shown to be  
 801 inducible both by flavonoids and plant host root exudates.  
 802 Similarly, Klonowska and collaborators found that *Cupriavi-*  
 803 *duis taiwanensis* LMG19424 and *Paraburkholderia phyma-*  
 804 *tum* STM815 RND systems are induced by *M. pudica* root  
 805 exudates (Klonowska et al. 2018). Our results suggest that  
 806 this system would also be important for the growth of *Cupri-*  
 807 *avidus* sp. UYMMa02A in the presence of *M. pudica* root  
 808 exudates. As mentioned, one role for these efflux systems is  
 809 the detoxification of harmful compounds. In that sense, the  
 810 RAST annotation server indicates that the identified protein  
 811 would be a membrane fusion protein of the CzcB family,  
 812 which is part of the CzcCBA Heavy metal efflux (HME)  
 813 RND system (Janssen et al. 2010). CzcCBA systems were  
 814 first described in *C. metallidurans* CH34 and shown to con-  
 815 fer resistance to Co, Zn, and Cd. Our evidence suggests that  
 816 *Cupriavidus* sp. UYMMa02A activates the extrusion of met-  
 817 als from its cytoplasm, perhaps preventing the formation of  
 818 reactive oxygen species (ROS). The increase in *Cupriavidus*  
 819 sp. UYMMa02A peroxiredoxin levels support the hypothesis  
 820 that ROS are formed during this interaction. Peroxiredoxin  
 821 is a periplasmic protein implicated in the detoxification of  
 822 ROS and peroxynitrite, also detected in *Rhizobium legu-*  
 823 *minosarum*, *C. taiwanensis*, and *P. phymatum* rhizobial  
 824 strains growing in the presence of root exudates (Ramachan-  
 825 dran et al. 2011; Klonowska et al. 2018). Another stress-  
 826 related induced protein is cyclophilin. Cyclophilins are

Peptidyl-prolyl cis/trans isomerases (PPIase, EC: 5.2.1.8) 827  
 enzymes found in all kingdoms of life. Since these proteins 828  
 catalyze a rate-limiting step in protein folding, they play 829  
 a critical role in protein homeostasis. Diverse studies have 830  
 demonstrated the participation of these proteins in signal 831  
 transduction, biofilm formation, motility, and adaptation to 832  
 stress (Skagia et al. 2016; Dimou et al. 2017; Thomloui 833  
 et al. 2017). Thomloui and collaborators showed that the 834  
 heterologous expression of the two cyclophilins isoforms 835  
 of *Sinorhizobium meliloti* 1021 in *E. coli* enhance bacterial 836  
 survival under stress condition, supporting the role of these 837  
 proteins in stress adaptation in bacteria. In addition, a PPIase 838  
 mutant in *Azorhizobium caulinodans* ORS571 impairs its 839  
 symbiosis with *Sesbania rostrata*, reducing nodule size and 840  
 completely abolishing its nitrogen fixation ability (Suzuki 841  
 et al. 2007). Along with the increase in the protein levels of 842  
 the Efflux RND periplasmic adaptor subunit, peroxiredoxin, 843  
 and PPIase, we also observed an increase in the universal 844  
 stress protein A (UspA) levels. Universal stress proteins are 845  
 small cytoplasmic bacterial proteins whose expression is 846  
 enhanced when the cell is exposed to diverse stress agents 847  
 and has been implicated in cell survival during prolonged 848  
 exposure to stress conditions (Nyström and Neidhardt 1994). 849  
 Induced expression of genes encoding proteins of this fam- 850  
 ily has been observed during *Rhizobium leguminosarum* 851  
 growing in the rhizosphere of pea, alfalfa, and sugar beet 852  
 (Ramachandran et al. 2011), as well as in *C. taiwanensis* 853  
 and *P. phymatum* growing in the presence of *M. pudica* root 854  
 exudates (Klonowska et al. 2018). Altogether, the evidence 855  
 presented here strongly suggests that during the first steps 856  
 of the symbiosis, *Cupriavidus* sp. UYMMa02A is under 857  
 considerable stress pressure, a common feature in rhizobia- 858  
 legumes symbiosis. 859

860 Finally, we were able to detect the induction of proteins  
 861 with the potential to transduce host-secreted signals, such as  
 862 the protein kinase PrkA protein and the Nucleotide dinkinase  
 863 (NdK) protein. PrkA is a member of the conserved serine/  
 864 threonine protein kinase family widely distributed among  
 865 Bacteria, Archaea, and Eukarya (Stancik et al. 2018). Ser-  
 866 ine/Threonine kinases (STKs) act in concert with Serine/  
 867 Threonine phosphatase (STPs) to introduce or remove phos-  
 868 phate modifications in proteins at these residues. Revers-  
 869 ible protein phosphorylation is one of the main mechanisms  
 870 allowing bacteria to respond to environmental stimuli. Post-  
 871 translational phosphorylation/dephosphorylation influences  
 872 the activity of modified proteins by inducing conformational  
 873 changes and regulating protein–protein interactions. Thus,  
 874 STKs and STPs influence many different signal transduction  
 875 pathways in bacteria. In *Rhizobium leguminosarum*, disrup-  
 876 tion of the *pssZ* gene, encoding an STK, impacts exopolysac-  
 877 charide synthesis, surface properties, and symbiosis with  
 878 clover (Lipa et al. 2018). Despite this example, very few  
 879 studies address the role of STKs in the symbiosis between

rhizobia and legumes. The induction of the *Cupriavidus* sp. UYMMa02A PrkA in the presence of the host plant *Mimosa pudica*, suggests that this STK could have an important role during the initial steps of the symbiotic interaction and demands additional studies to determine its precise role.

On the other hand, Ndk is a housekeeping enzyme whose primary role is maintaining the cellular homeostasis of nucleoside triphosphate (NTP) and their deoxy derivatives (dNTPs) pools by catalyzing the reversible  $\gamma$ -phosphate transfer from NTPs (or dNTPs) to NDPs (or dNDPs) (Berg and Joklik 1953). In bacteria, the transfer of high-energy phosphates occurs by a ping-pong mechanism that involves the formation of a phosphor-histidine intermediate at a conserved histidine residue (Lascu and Gonin 2000). Moreover, it has been shown that His-Phosphorylated Ndk can phosphorylate other proteins at histidine residues modulating their activities, and affecting a myriad of bacterial processes (Lu et al. 1996; Attwood and Wieland 2015). For example, the *E. coli* Ndk can transfer its phosphate to the sensor proteins EnvZ and CheA, and then the phosphorylated kinases transfer the high-energy phosphate to their cognate response regulators OmpR and CheY, respectively, which are implicated in osmosis and chemical sensing (Lu et al. 1996). In other bacteria Ndk homologs have been implicated in the regulation of biofilms formation, the function of type 3 secretion systems, the modulation of quorum sensing, and the response to oxidative stress, playing a critical role in bacteria and host interactions (Yu et al. 2017). Interestingly, in some bacteria, Ndk can also be found extracellular and membrane-associated. In *P. aeruginosa*, it has been observed that membrane-associated Ndk correlates with the status of bacterial growth (Shankar et al. 1996). Analysis of the *Cupriavidus* sp. UYMMa02A Ndk sequence suggests that this protein could have both intracellular and periplasmic locations. The results presented here, suggest that this protein would be involved in the interaction between the rhizobial *Cupriavidus* sp. UYMMa02A and the plant host *Mimosa pudica*. Further experiments are needed to determine the exact role of this protein in the interaction, as the role of Ndk in beneficial plant-bacteria interaction has not been studied in detail.

## Conclusions

The genome of *Cupriavidus* sp. strain UYMMa02A encodes a conserved symbiotic island that includes a complete *nod-DBCIJHASUQ* gene cluster with a nod-box sequence in the promoter region of *nodB*. However, no induction of the *Cupriavidus* sp. UYMMa02A *nod* genes was evidenced in response to pure flavonoids or *Mimosa* spp. root exudates. These results suggest that *Cupriavidus* sp. UYMMa02A may employ Nod-independent mechanisms to establish

symbiosis. Using a quantitative proteomic approach, we detected significant proteomic changes in *Cupriavidus* sp. UYMMa02A when exposed to flavonoids or root exudates. Twenty-four differentially expressed proteins were identified covering diverse bacterial processes ranging from basic metabolism and transport functions to stress response and signal transduction. In the presence of the plant host, the major bacterial responses were related to amino acid metabolism and oxidative stress, which are common features in many rhizobia-legume interactions. Besides this, the increased levels of the proteins PrkA and Ndk proteins during the co-culture conditions indicated the involvement of these versatile proteins in the symbiotic interaction. While further research is necessary to determine the precise roles of the identified proteins, our study presents a new model for interrogating the symbiotic interaction between beta-rhizobia and plant hosts.

**Funding** Funding was provided by Agencia Nacional de Investigación e Innovación (grant no. FCE\_1\_2014\_1\_104338, FCE\_1\_2017\_1\_136082, FCE\_1\_2019\_1\_156520), Programa de desarrollo de las ciencias básicas, PEDECIBA (grant no. 2018), and FONTAGRO (grant no. ID 30).

## References

- Amadou C, Pascal G, Mangenot S (2008) Genome sequence of the  $\beta$ -rhizobium *Cupriavidus taiwanensis* and comparative genomics of rhizobia. *Genome Res* 18:1472–1483
- Andam CP, Mondo SJ, Parker MA (2007) Monophyly of *nodA* and *nifH* genes across Texan and Costa Rican populations of *Cupriavidus nodula* symbionts. *Appl Environ Microbiol* 73:4686–4690
- Andrews M, Andrews ME (2017) Specificity in legume-rhizobia symbioses. *Int J Mol Sci* 18:705
- Attwood PV, Wieland T (2015) Nucleoside diphosphate kinase as protein histidine kinase. *Naunyn-Schmiedeberg's Arch Pharmacol* 388:153–160
- Aziz RK, Bartels D, Best AA, DeJongh M, Disz T, Edwards RA et al (2008) The RAST server: rapid annotations using subsystems technology. *BMC Genom* 9:75
- Bellés-Sancho P, Liu Y, Heiniger B, von Salis E, Eberl L, Ahrens CH et al (2022) A novel function of the key nitrogen-fixation activator NifA in beta-rhizobia: repression of bacterial auxin synthesis during symbiosis. *Front Plant Sci*. <https://doi.org/10.3389/fpls.2022.991548>
- Berg P, Joklik WK (1953) Transphosphorylation between nucleoside polyphosphates. *Nature* 172:1008–1009
- Bontemps C, Elliott GN, Simon MF, Dos Reis Júnior FB, Gross E, Lawton RC et al (2010) Burkholderia species are ancient symbionts of legumes. *Mol Ecol* 19:44–52
- Bradford MM (1976) A rapid and sensitive method for the quantitation of microgram quantities of protein utilizing the principle of protein-dye binding. *Anal Biochem* 72:248–254
- Capela D, Carrere S, Batut J (2005) Transcriptome-based identification of the *Sinorhizobium meliloti* NodD1 regulon. *Appl Environ Microbiol* 71:4910–4913
- Caporali S, De Stefano A, Calabrese C, Giovannelli A, Pieri M, Savini I et al (2022) Anti-inflammatory and active biological

- properties of the plant-derived bioactive compounds luteolin and luteolin 7-glucoside. *Nutrients* 14:1–19
- 986  
987  
988 Chen CC, Chou TL, Lee CY (2000) Cloning, expression and character-  
989 ization of L-aspartate  $\beta$ -decarboxylase gene from *Alcaligenes*  
990 *faecalis* CCRC 11585. *J Ind Microbiol Biotechnol* 25:132–140
- 991 Chen W, Laevens S, Lee T, Coenye T, Vos PD, Mergeay M, Van-  
992 damme P (2001) *Ralstonia taiwanensis* sp. nov., isolated from  
993 root nodules of *Mimosa* species and sputum of a cystic fibrosis  
994 patient. *Int J Syst Evol Microbiol* 51:1729–1735
- 995 Chen W-M, Moulin L, Bontemps C, Vandamme P, Béna G,  
996 Boivin-Masson C (2003) Legume symbiotic nitrogen fixation  
997 by beta-proteobacteria is widespread in nature. *J Bacteriol*  
998 185:7266–7272
- 999 Chen W-M, Prell J, James EK, Sheu D-S, Sheu S-Y (2012) Biosynthe-  
1000 sis of branched-chain amino acids is essential for effective sym-  
1001 bioses between betarhizobia and *Mimosa pudica*. *Microbiology*  
1002 158:1758–1766
- 1003 Cheng C-S, Su C-W, Chang W-C, Huang K-C (2014) CELLO2GO: a  
1004 web server for protein subCELLular LOCALization prediction with  
1005 functional gene ontology annotation. *PLoS ONE* 9:99368
- 1006 Cunnac S, Boucher C, Genin S (2004) Characterization of the cis-  
1007 acting regulatory element controlling HrpB-mediated activation  
1008 of the type III secretion system and effector genes in *Ralstonia*  
1009 *solanacearum*. *J Bacteriol* 186:2309–2318
- 1010 Dall'Agnol RF, Bournaud C, de Faria SM, Bena G, Moulin L, Hungria  
1011 M (2017) Genetic diversity of symbiotic Parabruckholderia spe-  
1012 cies isolated from nodules of *Mimosa pudica* (L.) and *Phaseolus*  
1013 *vulgaris* (L.) grown in soils of the Brazilian Atlantic Forest (Mata  
1014 Atlantica). *FEMS Microbiol Ecol*. <https://doi.org/10.1093/femsec/fix027>
- 1015  
1016 de Campos SB, Lardi M, Gandolfi A, Eberl L, Pessi G (2017) Muta-  
1017 tions in two *Parabruckholderia phymatum* type VI secretion sys-  
1018 tems cause reduced fitness in interbacterial competition. *Front*  
1019 *Microbiol* 8:2473
- 1020 De Meyer SE, Fabiano E, Tian R, Van Berkum P, Seshadri R, Reddy  
1021 T et al (2015a) High-quality permanent draft genome sequence  
1022 of the *Parapiptadenia rigida*-nodulating *Cupriavidus* sp. strain  
1023 UYPR2.512. *Stand Genom Sci* 10:13
- 1024 De Meyer SE, Parker M, Van Berkum P, Tian R, Seshadri R, Reddy  
1025 TBK et al (2015b) High-quality permanent draft genome sequence  
1026 of the *Mimosa asperata*-nodulating *Cupriavidus* sp. strain AMP6.  
1027 *Stand Genomic Sci* 10:9–11
- 1028 De Meyer SE, Briscoe L, Martínez-Hidalgo P, Agapakis CM, de-Los  
1029 Santos PE, Seshadri R et al (2016) Symbiotic *Burkholderia* spe-  
1030 cies show diverse arrangements of nif/fix and nod genes and lack  
1031 typical high-affinity cytochrome cbb3 oxidase genes. *Mol Plant*  
1032 *Microbe Interact* 29:609–619
- 1033 diCenzo GC, Zamani M, Checucci A, Fondi M, Griffiths JS, Finan  
1034 TM, Mengoni A (2019) Multidisciplinary approaches for studying  
1035 rhizobium–legume symbioses. *Can J Microbiol* 65:1–33
- 1036 Dimou M, Venferaki A, Katinakis P (2017) Microbial cyclophilins:  
1037 specialized functions in virulence and beyond. *World J Microbiol*  
1038 *Biotechnol* 33:1–8
- 1039 dos Reis FB, Simon MF, Gross E, Boddey RM, Elliott GN, Neto NE  
1040 et al (2010) Nodulation and nitrogen fixation by *Mimosa* spp.  
1041 in the Cerrado and Caatinga biomes of Brazil. *New Phytol*  
1042 186:934–946
- 1043 Dunn MF, Ramírez-Trujillo JA, Hernández-Lucas I (2009) Major roles  
1044 of isocitrate lyase and malate synthase in bacterial and fungal  
1045 pathogenesis. *Microbiology* 155:3166–3175
- 1046 Estrada-delossantos P, Palmer M, Chávez-Ramírez B, Beukes C, Steen-  
1047 kamp ET, Briscoe L et al (2018) Whole genome analyses suggests  
1048 that *Burkholderia sensu lato* contains two additional novel genera  
1049 (*Mycetohabitans* gen. nov., and *Trinickia* gen. nov.): implications  
1050 for the evolution of diazotrophy and nodulation in the Burkholde-  
1051 riaceae. *Genes* (basel). 9:389
- Fagorzi C, Bacci G, Huang R, Cangioli L, Checucci A, Fini M et al  
(2021) Nonadditive transcriptomic signatures of genotype-by-gen-  
type interactions during the initiation of plant-rhizobium sym-  
biosis. *mSystems*. <https://doi.org/10.1128/mSystems.00974-20>
- Gambino M, Cappitelli F (2016) Mini-review: biofilm responses to  
oxidative stress. *Biofouling* 32:167–178
- Garau G, Yates RJ, Deiana P, Howieson JG (2009) Novel strains of  
nodulating Burkholderia have a role in nitrogen fixation with  
papilionoid herbaceous legumes adapted to acid, infertile soils.  
*Soil Biol Biochem* 41:125–134
- Gehlot HS, Tak N, Kaushik M, Mitra S, Chen W-M, Poweleit N et al  
(2013) An invasive *Mimosa* in India does not adopt the symbionts  
of its native relatives. *Ann Bot* 112:179–196
- Gil M, Lima A, Rivera B, Rossello J, Urdániz E, Cascioferro A et al  
(2019) New substrates and interactors of the mycobacterial serine/  
threonine protein kinase PknG identified by a tailored interac-  
tomic approach. *J Proteom* 192:321–333
- Giraud E, Moulin L, Vallenet D, Barbe V, Cytryn E, Avarre J-C et al  
(2007) Legumes symbioses: absence of Nod genes in photosyn-  
thetic bradyrhizobia. *Science* 316:1307–1312
- Gourion B, Berrabah F, Ratet P, Stacey G (2015) Rhizobium-legume  
symbioses: the crucial role of plant immunity. *Trends Plant Sci*  
20:186–194
- Guha S, Molla F, Sarkar M, Ibañez F, Fabra A, DasGupta M (2022)  
Nod factor-independent “crack-entry” symbiosis in dalbergoid  
legume *Arachis hypogaea*. *Environ Microbiol* 24:2732–2746
- Howieson JG, Robson AD, Ewing MA (1993) External phosphate and  
calcium concentrations, and Ph, but not the products of rhizobial  
nodulation genes, affect the attachment of rhizobium meliloti to  
roots of annual medics. *Soil Biol Biochem* 25:567–573
- Howieson JG, De Meyer SE, Vivas-Marfisi A, Ratnayake S, Ardley JK,  
Yates RJ (2013) Novel *Burkholderia* bacteria isolated from *Leb-  
eckia ambigua*—a perennial suffruticose legume of the fynbos.  
*Soil Biol Biochem* 60:55–64
- Huergo LF, Dixon R (2015) The emergence of 2-oxoglutarate as a  
master regulator metabolite. *Microbiol Mol Biol Rev* 79:419–435
- Huerta-Cepas J, Szklarczyk D, Forslund K, Cook H, Heller D, Walter  
MC et al (2016) eggNOG 4.5: a hierarchical orthology framework  
with improved functional annotations for eukaryotic, prokaryotic  
and viral sequences. *Nucleic Acids Res* 44:286–293
- Hungria M, Joseph CM, Phillips DA (1991) Rhizobium nod gene  
inducers exuded naturally from roots of common bean (*Phaseolus  
vulgaris* L.). *Plant Physiol* 97:759–764
- Iriarte A, Platero R, Romero V, Fabiano E, Sotelo-Silveira JR (2016)  
Draft genome sequence of *Cupriavidus* UYMMa02A, a novel  
beta-rhizobium species. *Genome Announc* 4:e01258–e1316
- Janczarek M, Rachwał K, Cieśla J, Ginalska G, Bieganski A (2015a)  
Production of exopolysaccharide by *Rhizobium leguminosarum*  
bv. trifolii and its role in bacterial attachment and surface prop-  
erties. *Plant Soil* 388:211–227
- Janczarek M, Rachwał K, Marzec A, Grządziel J, Palusińska-Szyszk M  
(2015b) Signal molecules and cell-surface components involved  
in early stages of the legume–rhizobium interactions. *Appl Soil  
Ecol* 85:94–113
- Janssen PJ, Van Houdt R, Moors H, Monsieurs P, Morin N, Michaux A  
et al (2010) The complete genome sequence of cupriavidus metal-  
ludurans strain CH34, a master survivalist in harsh and anthropo-  
genic environments. *PLoS ONE* 5:e10433
- Jiménez-Guerrero I, Acosta-Jurado S, del Cerro P, Navarro-Gómez P,  
López-Baena F, Ollero F et al (2017) Transcriptomic studies of  
the effect of nod gene-inducing molecules in rhizobia: different  
weapons, one purpose. *Genes* (basel). <https://doi.org/10.3390/genes9010001>
- Kakimoto T, Kato J, Shibata T, Nishimura N, Chibata I (1969) Crys-  
talline L-aspartate  $\beta$ -decarboxylase of *Pseudomonas dacunhae*. *J  
Biol Chem* 244:353–358

- 1118 Klonowska A, Chaintreuil C, Tisseyre P, Miché L, Melkonian R,  
1119 Ducouso M et al (2012) Biodiversity of *Mimosa pudica* rhizobial  
1120 symbionts (*Cupriavidus taiwanensis*, *Rhizobium mesoamerica-*  
1121 *num*) in New Caledonia and their adaptation to heavy metal-rich  
1122 soils. *FEMS Microbiol Ecol* 81:618–635
- 1123 Klonowska A, Melkonian R, Miché L, Tisseyre P, Moulin L (2018)  
1124 Transcriptomic profiling of *Burkholderia phymatum* STM815,  
1125 *Cupriavidus taiwanensis* LMG19424 and *Rhizobium mesoameri-*  
1126 *canum* STM3625 in response to *Mimosa pudica* root exudates  
1127 illuminates the molecular basis of their nodulation competitive-  
1128 ness and symbiotic ev. *BMC Genom* 19:105
- 1129 Klonowska A, Moulin L, Ardley JK, Braun F, Gollagher MM, Zand-  
1130 berg JD et al (2020) Novel heavy metal resistance gene clusters  
1131 are present in the genome of *Cupriavidus neocaledonicus* STM  
1132 6070, a new species of *Mimosa pudica* microsymbiont isolated  
1133 from heavy-metal-rich mining site soil. *BMC Genom* 21:214
- 1134 Kornberg HL (1966) The role and control of the glyoxylate cycle in  
1135 *Escherichia coli*. *Biochem J* 99:1–11
- 1136 Kumar S, Stecher G, Tamura K (2016) MEGA7: molecular evolution-  
1137 arily genetics analysis version 7.0 for bigger datasets. *Mol Biol*  
1138 *Evol* 33:1870–1874
- 1139 Laemmli U (1970) Cleavage of structural proteins during the assembly  
1140 of the head of bacteriophage T4. *Nature* 227:680–685
- 1141 Lardi M, Liu Y, Purtschert G, de Campos SB, Pessi G (2017) Tran-  
1142 scriptome analysis of *Paraburkholderia phymatum* under nitrogen  
1143 starvation and during symbiosis with *Phaseolus vulgaris*. *Genes*  
1144 (basel). 8:389
- 1145 Lascu I, Gonin P (2000) The catalytic mechanism of nucleoside diphos-  
1146 phate kinases. *J Bioenerg Biomembr* 32:237–246
- 1147 Lemaire B, Dlodlo O, Chimphango S, Stirton C, Schrire B, Boatwright  
1148 JS et al (2015) Symbiotic diversity, specificity and distribution of  
1149 rhizobia in native legumes of the Core Cape Subregion (South  
1150 Africa). *FEMS Microbiol Ecol* 91:1–17
- 1151 Lindström K, Mousavi SA (2020) Effectiveness of nitrogen fixation in  
1152 rhizobia. *Microb Biotechnol* 13:1314–1335
- 1153 Lipa P, Vinardell JM, Kopicńska J, Zdybicka-Barabas A, Janczarek M  
1154 (2018) Mutation in the *pssZ* gene negatively impacts exopolysac-  
1155 charide synthesis, surface properties, and symbiosis of *Rhizobium*  
1156 *leguminosarum* bv. *trifolii* with clover. *Genes* (basel). 9:369
- 1157 Liu X, Wei S, Wang F, James EK, Guo X, Zagar C et al (2012)  
1158 *Burkholderia* and *Cupriavidus* spp. are the preferred symbi-  
1159 onts of *Mimosa* spp. in Southern China. *FEMS Microbiol Ecol*  
1160 80:417–426
- 1161 Liu Y, Bellich B, Hug S, Eberl L, Cescutti P, Pessi G (2020) the  
1162 exopolysaccharide cepacian plays a role in the establishment of  
1163 the *Paraburkholderia phymatum*—*Phaseolus vulgaris* symbiosis.  
1164 *Front Microbiol* 11:1600
- 1165 Lu Q, Park H, Egger LA, Inouye M (1996) Nucleoside-diphosphate  
1166 kinase-mediated signal transduction via histidyl-aspartyl phospho-  
1167 rylation systems in *Escherichia coli*. *J Biol Chem* 271:32886–32893
- 1168 Mailloux RJ, Bériault R, Lemire J, Singh R, Chénier DR, Hamel RD,  
1169 Appanna VD (2007) The tricarboxylic acid cycle, an ancient  
1170 metabolic network with a novel twist. *PLoS ONE* 2:e690
- 1171 Marchetti M, Capela D, Glew M, Cruveiller S, Chane-Woon-Ming B,  
1172 Gris C et al (2010) Experimental evolution of a plant pathogen  
1173 into a legume symbiont. *PLoS Biol* 8:e1000280
- 1174 Marchetti M, Catrice O, Batut J, Masson-Boivin C (2011) *Cupri-*  
1175 *avidus taiwanensis* bacteroids in *Mimosa pudica* Indeterminate  
1176 nodules are not terminally differentiated. *Appl Environ Microbiol*  
1177 77:2161–2164
- 1178 Martinez A, Kolter R (1997) Protection of DNA during oxidative  
1179 stress by the nonspecific DNA-binding protein Dps. *J Bacteriol*  
1180 179:5188–5194
- 1181 Masson-Boivin C, Giraud E, Perret X, Batut J (2009) Establishing  
1182 nitrogen-fixing symbiosis with legumes: how many rhizobium  
1183 recipes? *Trends Microbiol* 17:458–466
- Meleady P (2018) Two-dimensional gel electrophoresis and  
2D-DIGE. *Methods Mol Biol* 1664:3–14
- Miché L, Moulin L, Chaintreuil C, Contreras-Jimenez JL, Munive-  
Hernández JA, del Carmen Villegas-Hernandez M et al (2010)  
Diversity analyses of *Aeschynomene* symbionts in Tropical  
Africa and Central America reveal that nod-independent stem  
nodulation is not restricted to photosynthetic bradyrhizobia.  
*Environ Microbiol* 12:2152–2164
- Miller JH (1972) Assay of B-galactosidase In: Experiments in  
molecular genetics. Cold Spring Harbor Laboratory Press, Cold  
Spring Harbor
- Moskowitz GJ, Merrick JM (1969) Metabolism of poly-  
β-hydroxybutyrate. II. Enzymic synthesis of D-(-)-β-  
hydroxybutyryl coenzyme A by an enoyl hydase from *Rho-*  
*spirillum rubrum*. *Biochemistry* 8:2748–2755
- Moulin L, Klonowska A, Caroline B, Booth K, Vriezen JAC, Melko-  
nian R et al (2014) Complete genome sequence of *Burkholde-*  
*ria phymatum* STM815(T), a broad host range and efficient  
nitrogen-fixing symbiont of *Mimosa* species. *Stand Genom Sci*  
9:763–774
- Mozejko-Ciesielska J, Mostek A (2019) A 2D-DIGE-based proteomic  
analysis brings new insights into cellular responses of *Pseu-*  
*domonas putida* KT2440 during polyhydroxyalkanoates synthesis.  
*Microb Cell Fact* 18:1–13
- Nies DH (2003) Efflux-mediated heavy metal resistance in prokaryotes.  
*FEMS Microbiol Rev* 27:313–339
- Nyström T, Neidhardt FC (1994) Expression and role of the universal  
stress protein, UspA, of *Escherichia coli* during growth arrest.  
*Mol Microbiol* 11:537–544
- Oldroyd GED, Murray JD, Poole PS, Downie JA (2011) The rules of  
engagement in the legume-rhizobial symbiosis. *Annu Rev Genet*  
45:119–144
- Orban K, Finkel SE (2022) Dps is a universally conserved dual-action  
DNA-binding and ferritin protein. *J Bacteriol* 204:1–23
- Parker MA, Wurtz AK, Paynter Q (2007) Nodule symbiosis of invasive  
*Mimosa pigra* in Australia and in ancestral habitats: a comparative  
analysis. *Biol Invasions* 9:127–138
- Pereira-Gómez M, Ríos C, Zabaleta M, Lagurara P, Galvalisi U, Iccardi  
P et al (2020) Native legumes of the Farrapos protected area in  
Uruguay establish selective associations with rhizobia in their  
natural habitat. *Soil Biol Biochem* 148:107854
- Platero R, James EK, Rios C, Iriarte A, Sandes L, Zabaleta M et al  
(2016) Novel *Cupriavidus* strains isolated from root nodules  
of native Uruguayan *Mimosa* species. *Appl Environ Microbiol*  
82:3150–3164
- Prell J, Poole P (2006) Metabolic changes of rhizobia in legume nod-  
ules. *Trends Microbiol* 14:161–168
- Prell J, White JP, Bourdes A, Bunnewell S, Bongaerts RJ, Poole PS  
(2009) Legumes regulate *Rhizobium* bacteroid development and  
persistence by the supply of branched-chain amino acids. *Proc*  
*Natl Acad Sci USA* 106:12477–12482
- Ramachandran VK, East AK, Karunakaran R, Downie JA, Poole PS  
(2011) Adaptation of *Rhizobium leguminosarum* to pea, alfalfa  
and sugar beet rhizospheres investigated by comparative transcrip-  
tomics. *Genome Biol* 12:R106
- Rodríguez-Esperón MC, Eastman G, Sandes L, Garabato F, Eastman I,  
Iriarte A et al (2022) Genomics and transcriptomics insights into  
luteolin effects on the beta-rhizobial strain *Cupriavidus necator*  
UYPR2.512. *Environ Microbiol* 24:240–264
- Saad MM, Crèvecoeur M, Masson-Boivin C, Perret X (2012) The  
type 3 protein secretion system of *Cupriavidus taiwanensis* strain  
LMG19424 compromises symbiosis with *Leucaena leucocephala*.  
*Appl Environ Microbiol* 78:7476–7479
- Salehi B, Venditti A, Sharifi-Rad M, Kęrgiel D, Sharifi-Rad J, Durazzo  
A et al (2019) The therapeutic potential of Apigenin. *Int J Mol*  
*Sci* 20:1305

- 1250 Sambrook J, Fritsch EF, Maniatis T (1989) Molecular cloning: a laboratory manual 1280
- 1251 1281
- 1252 Santos MR, Marques AT, Becker JD, Moreira LM (2014) The 1282
- 1253 *Sinorhizobium meliloti* EmrR regulator is required for efficient 1283
- 1254 colonization of *Medicago sativa* root nodules. Mol Plant Microbe 1284
- 1255 Interact 27:388–399 1285
- 1256 Schlaman HRM, Okker RJH, Lugtenberg BJJ (1992) Regulation of 1286
- 1257 nodulation gene expression by nodD in rhizobia. J Bacteriol 1287
- 1258 174:5177–5182 1288
- 1259 Schmidt PE, Broughton WJ, Werner D (1994) Nod factors of 1289
- 1260 *Bradyrhizobium japonicum* and *Rhizobium* sp. NGR234 induce 1290
- 1261 flavonoid accumulation in soybean root exudate. Mol Plant 1291
- 1262 Microbe Interact 7:384–390 1292
- 1263 Shankar S, Kamath S, Chakrabarty AM (1996) Two forms of the 1293
- 1264 nucleoside diphosphate kinase of *Pseudomonas aeruginosa* 8830: 1294
- 1265 altered specificity of nucleoside triphosphate synthesis by the cell 1295
- 1266 membrane-associated form of the truncated enzyme. J Bacteriol 1296
- 1267 178:1777–1781
- 1268 Skagia A, Zografou C, Vezyri E, Venieraki A, Katinakis P, Dimou M 1297
- 1269 (2016) Cyclophilin PpiB is involved in motility and biofilm for- 1298
- 1270 mation via its functional association with certain proteins. Genes 1299
- 1271 Cells 21:833–851 1300
- 1272 Stancik IA, Šestak MS, Ji B, Axelson-Fisk M, Franjevic D, Jers C et al 1301
- 1273 (2018) Serine/threonine protein kinases from bacteria, archaea 1302
- 1274 and Eukarya share a common evolutionary origin deeply rooted 1303
- 1275 in the tree of life. J Mol Biol 430:27–32
- 1276 Suzuki S, Aono T, Lee KB, Suzuki T, Liu CT, Miwa H et al (2007) 1304
- 1277 Rhizobial factors required for stem nodule maturation and main- 1305
- 1278 tenance in *Sesbania rostrata*-*Azorhizobium caulinodans* ORS571 1306
- 1279 symbiosis. Appl Environ Microbiol 73:6650–6659
- Taulé C, Zabaleta M, Mareque C, Platero R, Sanjurjo L, Sicardi M 1280
- et al (2012) New betaproteobacterial *Rhizobium* strains able to 1281
- efficiently nodulate *Parapiptadenia rigida* (Benth.) Brenan. Appl 1282
- Environ Microbiol 78:1692–1700 1283
- Thomloudi E-E, Skagia A, Venieraki A, Katinakis P, Dimou M (2017) 1284
- Functional analysis of the two cyclophilin isoforms of *Sinorhizo-* 1285
- bium meliloti*. World J Microbiol Biotechnol 33:28 1286
- Wu PS, Yen JH, Kou MC, Wu MJ (2015) Luteolin and apigenin attenu- 1287
- ate 4-hydroxy-2-nonenal-mediated cell death through modulation 1288
- of UPR, Nrf2-ARE and MAPK pathways in PC12 cells. PLoS 1289
- ONE 10:1–23 1290
- Yu H, Rao X, Zhang K (2017) Nucleoside diphosphate kinase (Ndk): a 1291
- pleiotropic effector manipulating bacterial virulence and adaptive 1292
- responses. Microbiol Res 205:125–134 1293
- Zheng J, Wang R, Liu R, Chen J, Wei Q, Wu X et al (2017) The struc- 1294
- ture and evolution of beta-rhizobial symbiotic genes deduced from 1295
- their complete genomes. Immunome Res 13:131 1296
- Publisher's Note** Springer Nature remains neutral with regard to 1297
- jurisdictional claims in published maps and institutional affiliations. 1298
- Springer Nature or its licensor (e.g. a society or other partner) holds 1299
- exclusive rights to this article under a publishing agreement with the 1300
- author(s) or other rightsholder(s); author self-archiving of the accepted 1301
- manuscript version of this article is solely governed by the terms of 1302
- such publishing agreement and applicable law. 1303

|          |              |
|----------|--------------|
| Journal: | <b>42398</b> |
| Article: | <b>286</b>   |

## Author Query Form

**Please ensure you fill out your response to the queries raised below and return this form along with your corrections**

Dear Author

During the process of typesetting your article, the following queries have arisen. Please check your typeset proof carefully against the queries listed below and mark the necessary changes either directly on the proof/online grid or in the 'Author's response' area provided below

| Query               | Details Required   | Author's Response |
|---------------------|--|-------------------|
| <a href="#">AQ1</a> | Article title: Kindly check and confirm the edit made in the title.  |                   |
| <a href="#">AQ2</a> | Affiliations: Journal instruction requires a city and country for affiliations; however, city is missing in affiliations [1 to 5]. Please verify if the provided city are correct and amend if necessary.  |                   |
| <a href="#">AQ3</a> | Kindly note that (3-6) has been deleted in sentence "In beta-proteobacteria, the...". Please check and confirm.  |                   |
| <a href="#">AQ4</a> | Please provide reference for citations "Hanahan (1983) and Kessler et al. (1992)".   |                   |
| <a href="#">AQ5</a> | Kindly check and confirm the caption of tables 2 and 3".   |                   |
| <a href="#">AQ6</a> | Figure: Journal standard requires that the first figure referenced in the manuscript text should be Figure 1, the second, Figure 2, etc. However, the original sequence of figure citations [9, 8] is out of order. Figure images and citations were reordered so that they are cited in consecutive order. Please check if action taken is appropriate. |                   |
| <a href="#">AQ7</a> | Kindly check and confirm the funding statement.  |                   |
| <a href="#">AQ8</a> | Inclusion of a data availability statement is preferred for this journal. If applicable, please provide one.   |                   |
| <a href="#">AQ9</a> | As References Jiménez-Guerrero et al., 2017 and Jiménez-Guerrero et al., 2018 are same, we have deleted the duplicate reference and renumbered accordingly. Please check and confirm.  |                   |